ISSN 0280-5316
ISRN LUTFD2/TFRT--5699--SE

Modelling of Crankcase Gas Behaviour in a Heavy-Duty Diesel Engine

Pontus Avergård
Fredrik Lindström

Department of Automatic Control
Lund Institute of Technology
January 2003

Department of Automatic Control
Lund Institute of Technology
Box 118
SE-221 00 Lund Sweden

Document name
MASTER THESIS

Date of issue
January 2003

Document Number
ISRN LUTFD2/TFR--5699--SE

Author(s)
Pontus Avergård and Fredrik Lindström

Supervisor
Rolf Johansson, LTH
Mats-Örjan Pogén, Haldex

Sponsoring organization

Title and subtitle
Modelling of Crankcase Gas Behaviour in a Heavy-Duty Diesel Engine (Modellering av vevhusgasbildning I en tung dieselmotor).

Abstract
The origin of many environmental and health hazardous emissions from diesel engines are the crankcase gases. Since no regulations of the emission levels from the crankcase have existed in the past, no attention has been paid to cleaning crankcase gases. New regulations are coming up and they will all demand lower emissions from the engine.
This has lead to the introduction of the Alfdex separator. The Alfdex separator is built to separate oil droplets and soot from the crankcase gases.
In the research work made in this master thesis, we have investigated the possibilities to model the crankcase gases with respect to flow rate and oil content with some parameters of the engine. The model could then be used as an input to a controller that controls the separator speed. Since the test engine used here is old and is not in production anymore, the idea of the modelling is to find more general characteristics rather than specifics for the tested engine.
The work made in this master thesis shows that the crankcase gas flow rate can be modelled in a good way. The identifying process done here is accomplished by field tests on a Volvo bus equipped with a TD123E motor, which is a 6 cylinder, 12 litres, turbocharged diesel engine. Since no prior testing had been made, the project involved much practical work such as test rig building, mounting on the bus etc. The measurements on crankcase gases have been made both at stationary modes and dynamically.
The project also involves measurements of the oil content in crankcase gases. These measurements have been made at steady state, with no possibility to investigate the dynamic behaviour of the oil aerosol. The tests made on the size distribution of oil in the crankcase gases gives a hint to the future development of a controller.

Keywords
crankcase ventilation, blow-by, subspace modelling, oil mist

Classification system and/or index terms (if any)

Supplementary bibliographical information

ISSN and key title
0280-5316

ISBN

Language
English

Number of pages
60

Recipient's notes

Security classification

The report may be ordered from the Department of Automatic Control or borrowed through:
University Library 2, Box 3, SE-221 00 Lund, Sweden
Fax +46 46 222 44 22 E-mail ub2@ub2.se

Sammanfattning

Ursprunget till många miljö- och hälsoskadliga dieselavgaser är vevhusgaserna. Eftersom det tidigare inte funnits några bestämmelser på utsläpps nivåer har ingen större tonvikt lagts på vevhusgaserna. Nya bestämmelser angående utsläppsnivåer introduceras inom en snar framtid. Detta har lett till introduktionen av Alfdex-separatorn. Alfdex-separatorn är framtagen för att separera oljedroppar och sot från vevhusgaserna.

Vi har i detta examensarbete undersökt möjligheten att modellera vevhusgasflödet med hjälp av inparametrar från motorn. Modellen kan senare användas som insignal till en styrande motor i separatorn. Testerna som gjorts är utförda på en motormodell som inte längre är i produktion vilket innebär att vi har inriktat oss på generell karakteristik.

Detta arbete visar att det är möjligt att modellera vevhusgaserna med bra resultat. Identifieringsprocessen är gjord på en motor av märket Volvo TD123E, vilket är en 6 cylindrig 12 liters dieselmotor med turbo. Då det inte fanns några tidigare tester gjorda på vevhusgaserna så har en del av tiden inneburit praktiskt arbete, t.ex. byggandet och monteringen av testriggen. Tester har utförts både i stationäritet och dynamiskt.

Arbetet har också innefattat mätningar på oljedimman i vevhusgaserna. Dessa mätningar har skett i stationäritet utan möjlighet att undersöka eventuell dynamik. Mätningarna gjorda på oljedimmans storleksfördelning ger en fingervisning till framtida utveckling av en regulator.

Preface

We first set out to make a controller for the Alfdex oil mist separator. Since then, the focus of the master thesis has shifted somewhat towards examination of crankcase gases. We hope that this change of focus has given some extra value to the work and better understanding of the behaviour of crankcase gases.

Our supervisor at Haldex Brake Products, Mats-Örjan Pogén, has been a good discussion partner throughout the project. We wish to thank Haldex and Alfa Laval for giving us the opportunity to do this master thesis in such an interesting and important area of research.

Professor Rolf Johansson has been our supervisor and examiner at the Department of Automatic Control, Lund Institute of Technology. He has provided suggestions of system identification algorithms and general support on the topic of system identification and measurements.

Dr. Anders Gudmundsson at the Department of Ergonomics and Aerosol Technology at LIT provided particle size measuring equipment and great guidance in the handling of the equipment.

All personnel at the Haldex Brake Products lab have been very helpful. Without all their help we would not have been able to perform our tests. Especially we wish to thank Fredrik Rennstam for his safe driving skills and help with the measuring equipment. Peter was a great help in the construction of the test rig.

Finally we want to thank Lars Erlandsson at Volvo Truck Corporation for the informative meeting, which gave the whole project a flying start.

Landskrona in January, 2003

Pontus Avergård Fredrik Lindström

Table of Contents

1 Introduction

Blow-by gas will arise during the use of any kind of combustion engine. Blow-by is the leakage from the combustion chamber to the crankcase. Blow-by gas consist of the desired residual products in a combustion process, namely water and carbon dioxide, but it also contains substances like unburned fuel, NO_x and carbon monoxide. Besides the combustion process remnants there are also a substantial amount of oil aerosol in the blow-by gas. The blow-by gas on many modern heavy-duty diesel engines is let out directly to the atmosphere causing environmental damage. This kind of system is called open crankcase ventilation and it is only allowed on heavy-duty diesel engines. Otto engines have regulations on closed crankcase ventilation, which means that the blow-by gas is led back to the inlet manifold. This system does not work as well on turbocharged engines as on naturally aspirated. The drawback with open crankcase ventilation is of course the environmental influence and also the oil consumption. The currently used system needs regular oil refills and with a closed loop system the interval between these refills could be extended.

The upcoming regulations on vehicles with heavy-duty diesel engines have a new concept of measuring emissions. The focus is shifting from tailpipe emissions to vehicle emissions. This means that the crankcase ventilation system no longer can be an open system. It must be a closed system and to make this possible the gases must first be cleaned from oil. Alfa-Laval has developed a disc stack centrifugal separator (cf. Appendix C) that is able to separate particles from gases and they have further developed this product together with Haldex.

1.1 Background

During operation of a combustion engine a gas leakage from the combustion chamber down to the crankcase occurs. There is a large pressure difference in the two different spaces and, since the piston rings are not completely sealing, there will be a leakage. This leakage is called blow-by. To avoid pressurizing the crankcase and oil leakage due to broken gaskets (or in the worst case an explosion) these gases are led out from the crankcase.

1.1.1 Blow-By Characteristics

The blow-by flow originates not only from the combustion chamber, but also from other sources in the whole engine system. Around 60 % originates from the combustion process. The remaining 40 % descend from other sources [17].

1.1.1.1 Combustion Blow-By

The leakage from the combustion process mainly occurs during the compression and expansion stroke (cf. Figure 1-1) when the pressure reaches a maximum in the combustion chamber.

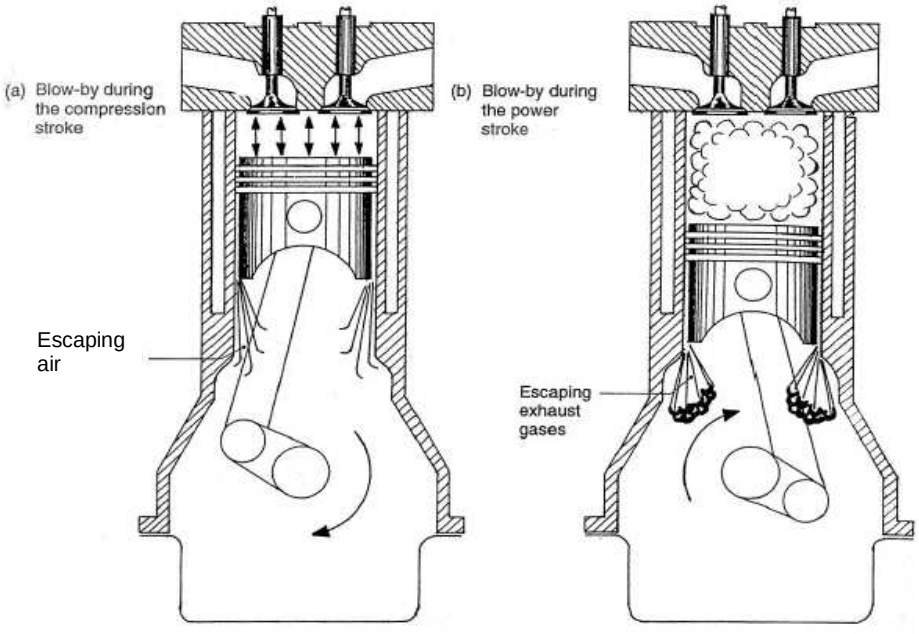

Figure 1-1 Blow-by during compression and expansion stroke [13].

When air from the intake manifold enters the combustion chamber, part of the volume enters the top land crevice (cf. Figure 1-2). This volume leaks down to the crankcase, partly around the piston rings due to high pressure, but also through the piston ring gap (cf. Figure 1-3) [14].

1.1.1.2 Other Sources

The other 40 % of the blow-by originates form a handful of different sources such as air compressor, turbo, turbo compounder and valve gear. All these blow-by sources have a connection to the crankcase. Either their own crankcase is in direct conjunction with it (e.g. air compressor) or they have lubricating channels that are connected to the oil sump [17]. The biggest contributor to the blow-by flow of these sources is the air compressor. A worn air compressor can leak as much as 180 l/min when charging, while a turbo leaks around 30 l/min. On the other hand, the leakage from the valve gear is insignificant on a turbocharged engine [17].

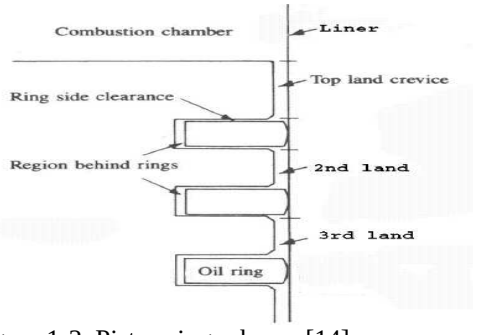

Figure 1-2 Piston ring scheme [14].

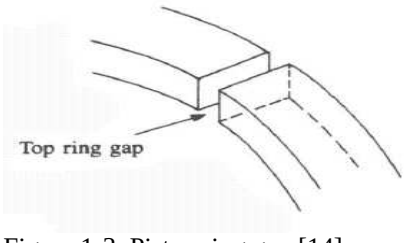

Figure 1-3 Piston ring gap [14].

1.1.1.3 Blow-By Flow Rate

The volume flow of the leakage compared to intake or exhaust flow shows that only 0,4-0,8 percent passes down to the crankcase in so-called blow-by [5]. The total amount of blow-by depends on different engine parameters such as load, engine speed, whether or not the air compressor is charging etc., but it also increases with the engines total operating time and it can vary a lot between different manufactures and models [9].

Special cases that can give high amounts of blow-by are exhaust brake and piston ring flutter. Piston ring flutter occurs when the pressure difference between the combustion chamber and the crankcase is not high enough to push the piston ring tightly onto the piston ring groove. The motion of the piston causes the piston ring to flutter in the groove. Typically, this occurs at some specific combination of engine speed and load.

The amount of blow-by is measured in a variety of ways and the values of measured blow-by are very different. The variety can be seen in Table 1-1 below.

Table 1-1 Different measurements of blow-by. The measurements have been done on engines with an output between 300–600 horsepower.

Measured value	*Reference*
10 – 30 l/min per cylinder	[6]
140 – 300 l/min	[5]
1120 l/min on a worn engine	[5]
0,5 l/min per rated engine horsepower	[5]

1.1.1.4 Blow-By Contents

Since most diesel engines of today uses a direct fuel injection in the combustion chamber, the gas that slips into the crevices between the piston and the cylinder wall is mainly air. Thus, the main part of the gas that leaks down to the crankcase is air but it also contains other particles such as residual deposits[1] (e.g. CO_2, CO, O_2, NO_x and H_2O), unburned fuel and soot [14]. The amount of unburned fuel can be as high as 2000 ppm [17].

When the gas leaks past the piston rings, the lubricating film of engine oil adhering to the pistons and cylinder faces are ripped away from the surface by the partially high flow rates and the oil is atomised[2] [6]. These superfine particles are called aerosols. Approximately 50 % of the oil aerosol forms around the piston rings and the cylinder wall. In addition, components of the engine oil with low boiling points vaporize and likewise lead to the formation of aerosols by condensation. Since the components of the engine such as the crankshaft is constantly rotating, oil splashes of varying droplet size builds up and are being mixed with the blow-by gas and drawn out of the crankcase. This leads to an unnecessary high consumption of oil [6].

The main portion of the droplets in the aerosol is found in an interval below 3 µm. Measurement has shown that more then 90 percent of the particles are found below 3 µm, 75 percent below 2 µm and 40 percent are less then 1 µm in particle diameter [5].

1.1.2 Previous Solutions and Upcoming Regulations

In the past there has been no regulations on crankcase emissions (on heavy-duty diesels), so a common solution on turbocharged, after cooled diesel engines is simply a downward directed draft tube that is vented directly to the atmosphere. This solution has been questioned as the environmental awareness has become higher. The crankcase emissions

[1] förbränningsrester
[2] finfördelas

contains substantial amount of PM[1], which can be as high as 0,7 g/bhp-hr [5] during idle conditions for modern engines.

The environmental associations around the world have recognized this problem and some regulations are being considered. Emission regulations in Japan, published by JAMA (Japan Automobile Manufactures Association, Inc.), require the use of closed systems starting in the year 2002 [5]. Other associations such as EPA (Environmental Protection Agency, U.S.) have proposed closed crankcase operation for the 2007 regulations [5]. In Europe the standard Euro IV, which will come into effect in 2005, will have higher demands on emissions, but it will not require closed crankcase ventilation [25].

1.1.3 Problems With Closed Crankcase Ventilation

An easy solution to the problem of reducing the pollution from crankcase ventilation is to close the system so that the crankcase gases are led back to the inlet manifold. This works quite well on naturally aspirated engines, but it does not work as well on those with turbocharger. The reason for this is that the oil droplets in the crankcase gas can damage the turbo and the intercooler. The problems that arise with this solution are:

- Oil contamination in the air conducts, especially in the intercooler where the heat transfer efficiency becomes lowered [6].
- Damage or lowered efficiency rate of the compressor wheel in the turbo [6]. The problem arises if the boost pressure is high enough. When compressing the air so that the temperature rises above 190°C there is a risk of coke deposits on the compressor blade [17]. This deteriorates the aerodynamic properties of the compressor and hence the efficiency.
- Negative effects on the emission of PM (Also a problem for engines without turbo charger) [9].

These problems have led to the development of cleaning devices for blow-by gases. Various solutions can be found on the market (filters, cyclones, electro static filters etc.), and they have been proven to be more or less efficient.

1.2 Purpose

A separator needs power to run, this power can be provided in different ways. Today a shovel is used either driven by the hydraulic oil system or by pressure air. A separator powered by an electrical engine would be controllable and hence power effective, but today's power system of 24 V does not have any extra energy to support additional auxiliary devices. But the power system on future engines will be upgraded to 42 V and then there will be a possibility to power the separator with an electrical engine. This will lead to more power savings since the degree of efficiency is higher on an electrical engine and also the lifetime of the separator would be extended if the speed could be controlled. This will eventually lead to lower costs. The purpose of this master thesis project is to investigate the origin of blow-by gases and find the controlling parameters so that a control structure can be developed. We have only found stationary data concerning blow-by flow and oil content in the literature. Dynamic behaviour needs to be investigated in

[1] Particulate matter (PM) is the general term used for a mixture of solid particles and liquid droplets found in the air. These particles can accumulate in the respiratory system and are associated with numerous health effects. [25]

order to design a control system. There is also an interest to investigate the size distribution of the oil mist, which can be useful when dimensioning the separator.

1.3 Delimitation

All tests have been carried out on a 12 litres turbocharged diesel engine. Since all engines are not alike the focus has been to identify general characteristics of the blow-by flow rate and oil aerosol rather than a control system implementation. No physical modelling has been made of the aerosol formation and blow-by flow. All blow-by flow results are based on measurements and identification of dynamic models. Only stationary test have been made of the oil droplet size distribution in the aerosol.

2 Method

All measurements have been executed on a Volvo bus with a TD123E 12 litres turbocharged engine manufactured in 1995. This engine probably has less blow-by flow than newer engines due to the fact that the maximum cylinder pressure limit has increased with better materials and construction [17]. The measuring equipment is described in detail below. The way the equipment was used for flow rate and particle size distribution measurements is described in 2.2.

2.1 Measuring Equipment

There have been no earlier tests on crankcase gases at Haldex prior to this one so a test set-up had to be built. The division of Ergonomics and Aerosol Technology at Lund Institute of Technology provided equipment such as cascade impactor, pump, part flow extraction probe and scales. Other equipment such as couplings was made at Haldex.

2.1.1 Flow Meters

Four different flow meters have been used during the experiments, three of which were variable area flow meters. The variable area flow meter, also known as rotameter, operates by a simple floating body principle. A float in a vertical tube maintains a dynamic equilibrium between upward forces (fluid stream) and downward forces (gravitational). The tube area increases with the height and the height of the float is a measure of the fluid flow through the tube.

Table 2-1 Variable area flow meters used during experiments

	Model	*Range*	*Output*	*Use*
1	Fisher Porter 10A5480	0-200 dm^3/min (100°C, 1013 hPa)	4-20 mA	blow-by flow measurement
2	Rota	2-40 dm^3/min (20°C, 1013 hPa)	none	calibration of cascade impactor flow
3	Asametro ES-2800/H	2500-25000 dm^3/h (20°C, 1013 hPa)	none	blow-by flow measurement

Flow meter 1 was calibrated for 100°C and $1.013 \cdot 10^5$ Pa. The measured flow has to be corrected for gas pressure and temperature according to

$$Q = Q_{meas} \sqrt{\frac{373.15}{T_G}} \sqrt{\frac{p}{1.013}} \tag{2.1}$$

T_G: gas temperature [K]

p_G: absolute gas pressure [$Pa \cdot 10^5$]

The variable area flow meters are sensitive to inclination. Although the floats in the large flow meters (1 and 3) were damped, the damping was quite poor.

The fourth flow meter was a Testo turbine inserted in a tube with 12 mm inner diameter. The turbine was connected to a Testo 400 unit, enabling sampling and monitoring of the flow velocity. The flow velocity range of the instrument was 0.4-60 m/s (2 - 400 dm^3/min).

2.1.2 Logger

The logging equipment Haldex uses is a LogBook 360. It is a 16-bit sampler with a memory capacity of 250 million data points and it has a sampling frequency range of up to 100 kHz depending on the number of calculations that are required in real-time.

Figure 2-1 Flow meter 2, a variable area flow meter.

2.1.3 Pump

The pump provided by LIT was an AC motor with an efficiency of 186 Watts and with the maximum rpm of 1425. To control the flow rate of the pump a needle valve was used to throttle the suction rate.

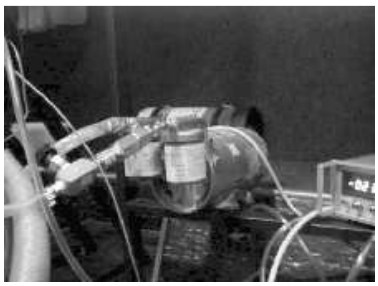

Figure 2-2 Pump

2.1.4 Isokinetic Part Flow Extraction Probe

Dr. Anders Gudmundsson at the division of Ergonomics and Aerosol Technology at Lund Institute of Technology provided the isokinetic part flow extraction probe. The isokinetic probe is necessary when a small gas flow should be sampled from a large flow without affecting the particle size distribution. The meaning of isokinetic is that the velocity and the direction of the gas flows are constant. A principal sketch of the isokinetic probe is shown in Figure 2-9.

Measurements done by Löffler [20] show that the deviation with regard to the mass concentration for over-isokinetic part flow extraction is smaller than the deviation for sub-isokinetic part flow extraction. On the other hand the deviation of the particle size distribution is negligible for both over- and sub-isokinetic part flow extraction. The explanation for the negligible influence on the particle size distribution is that the particles in the crankcase gas are small (0.3-4μm) [20]. In the over-isokinetic example this means that even the biggest particles are small enough to easily be drawn into the probe and hence not affect the particle size distribution negatively [11].

To avoid any turbulence at the tip of the probe or any kind of unwanted agglomeration between particles a so-called quiet length is introduced both before and after the probe opening. The total length of this quiet section should be at least 13 times the tube diameter. The length should be distributed as 10 times upstream and 3 times downstream [1]. To prevent agglomeration of particles when changing the probe tube diameter, the tube cone angle should not be larger than 10° [20].

The whole probe module was manufactured at Haldex. Four correction screws were used to adjust the probe to be in the middle of the module. In other measurements made by Krause [20], two pressure sensors were mounted exactly opposite to each other on the probe. Then the differential pressure was measured and the centre spot was adjusted.

2.1.5 Cascade Impactor

The cascade impactor is an instrument for measuring particle size distribution of an aerosol. It consists of several modules, each containing one or several nozzles and an impaction plate (cf. Figure 2-3). The measurements are done by gravimetrical analysis of the particles that hit the impaction plates. An aluminium foil is mounted on each impaction plate and the change of the foil weights are measured with accurate scales.

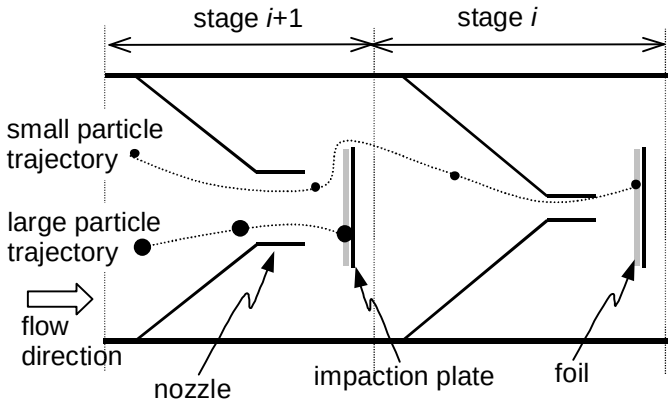

Figure 2-3 The cascade impactor operating principle and modular construction.

Each step in the cascade impactor is designed to separate 50 percent of the particles of a particular diameter $d_{50,i}$. This is done by choosing the diameter of the nozzles, the number of nozzles and the distance to the impaction plate. The properties of an impactor stage can be characterized by the dimensionless Stokes number, defined in equation (2.2). The Stokes number relates the stopping distance of a particle in a diverted gas flow to a characteristic dimension of the obstacle. The stopping distance is the time for a particle to reach its terminal velocity according to Stokes law. Once the Stokes number of an impactor stage is known, the 50 percent separation diameter can be calculated for the actual operation conditions from (2.2).

$$Stk_{50,i} = \frac{4\rho_p \Phi Cu_i d_{50,i}^2}{9\pi\eta_G W_i^3 N_i} = \frac{\rho_p U_i Cu_i d_{50,i}^2}{9\eta_G W} \quad [-] \tag{2.2}$$

where η_G is the dynamic viscosity

$$\eta_G = \frac{1.4687 \cdot 10^{-6}}{T_G + 113} T_G^{3/2} \quad [\text{Pas}] \tag{2.3}$$

and

$d_{50,i}$ [m]: diameter of particle with 50% separation in stage *i*
ρ_p [Kg/m^3]: particle density
Φ [m^3/s]: flow rate through the cascade impactor
W_i [m]: nozzle diameter in stage *i*
N_i [-]: number of nozzles in stage *i*
U_i [m/s]: initial velocity of the particles in stage *i*
$Stk_{50,i}$ [-]: Stokes number of the impactor stage *i*, experimentally determined
Cu_i [-]: Cunningham correction factor given by (2.4), explained below
T_G [K]: gas temperature

The Cunningham correction factor, defined in (2.4), is a correction of the Stokes number to account for particle slip. When the particle diameter is in the same range as the mean free path of the surrounding gas (e.g. 66 nm in air at 298 K, 1 atm), the gas can no longer be considered as a continuum. The gas velocity on the particle surface is not zero and the flow resistance due to the viscosity of the gas decreases. Hence, the Stokes number should be corrected upwards for small particles.

$$Cu = 1 + \frac{\lambda_G}{d_p}\left(2.514 + 0.80\exp\left(-0.55\frac{d_p}{\lambda_G}\right)\right) \tag{2.4}$$

$$\lambda_G = 2\frac{\eta_G}{p_G}\sqrt{\frac{\pi R T_G}{8M}} \tag{2.5}$$

where
d_p [m]: particle diameter
λ_G [m]: mean free path of particles given by (2.5)
p_G [Pa]: gas pressure
M [kg/mol]: molar gas mass = 28.96 kg/kmol

Adapted from [10], [11], [20] and [21].

2.1.5.1 Sensitivity Analysis

The choice of impactor nozzle diameter *W* is sensitive to experimental conditions. The sensitivity of the 50% separation diameter to a 10 % change in the temperature, the pressure of the gas and the volume flow are shown in Figure 2-4.

The curves suggest that there is only a small dependency on pressure in the expected pressure range. The pressure dependence is highest for small d_{50}. The dependence on temperature is stronger. Temperature measurements of the gas entering the cascade impactor has to be performed in order to draw conclusions on particle size distribution. The sensitivity analysis also indicates that the volume flow through the impactor has to be accurately measured.

2.1.5.2 Choice of Impactor Stages

The impactor we used was a copy of the ELPI (Electrical Low Pressure Impactor) described in [21]. The selection of stages was based upon the previous mass distribution measurements done by Krause [20] and the characterization of the ELPI done by Marjamäki et al [21]. The choice is done under the approximation that the distribution for the Volvo TD123E engine should have a similar appearance. The stages we chosen are seen in Table 2-2.

The pressure drop in each step was measured and the relative pressure drop was calculated. This information was used to calculate the mean free path of the gas (equation (2.5)) to be able to estimate the cut-off diameters from equation (2.2).

No back-up filter was used in the measurements.

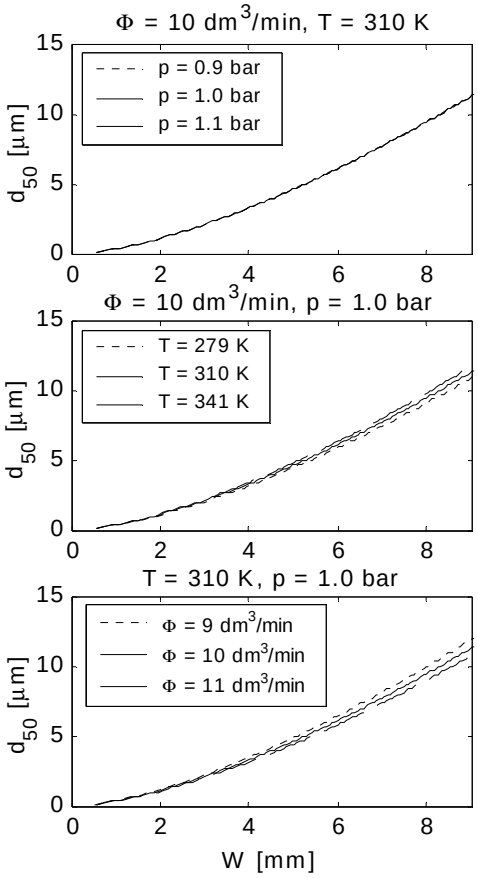

Figure 2-4 Sensitivity of d_{50} as a function of nozzle diameter W to a 10% change in gas pressure, temperature and flow rate.

2.1.5.3 Calibration of Flow Rate

To calibrate the 10 l/min flow rate through the impactor, we connected flow meter 2 upstream of the impactor. Then the suction rate was adjusted to approximately 10 l/min and the pressure after the cascade impactor was measured. When disconnecting the rotameter the suction rate of the pump was adjusted with the knowledge of the pressure drop over the rotameter. During the actual measurements the flow rate was adjusted to get the desired pressure and hence the desired flow rate after the impactor.

Table 2-2 Chosen impactor stages

Stage nbr[1]	d_{50} *[µm]*	*Relative pressure*[2] *[-]*	*Estimated flow velocities [m/s]*
11	4.29	1.000	6.9
9	1.72	0.997	13
8	1.02	0.995	22
7	0.662	0.989	28
5	0.295	0.957	93

[1] The numbers on the chosen stages refer to the numbers on the cascade impactor provided by LIT. The provided cascade impactor was a copy of the ELPI described in [21].
[2] Pressure relative to the pressure before the cascade impactor (i.e. at stage 11).

2.1.5.4 Evaluation of Measurements

The calculation of cumulative mass distribution from measured filter weights is done by (2.6) [20]. A backup filter that absorbs all remaining particles after the cascade impactor is needed to get full information of the particle size distribution.

$$Q_i = \frac{\sum_{k=0}^{i-1} m_k}{m_{tot}} \tag{2.6}$$

where

m_{tot} [kg]: total deposit on all foils and backup filter

m_k [kg]: deposit on foil k, numbering upstream, $k = n$ is the first stage of the impactor in the flow direction (that separates the larges particles), $k = 0$ is a backup filter

n [-]: number of impactor stages

Q_i can be interpreted as the portion of the mass that originates from particles smaller than or equal to $d_{50,i}$. The quantity 1 - Q_n is the portion of the mass that originates from particles larger than $d_{50,n}$.

Figure 2-5 The impactor stages that were used in the particle size measurements and foils with deposits.

2.1.6 Other Equipment

Other equipment used was standard bimetal thermocouples, velocity radar, and a Sartorius 2444 scale with 0.01 mg precision.

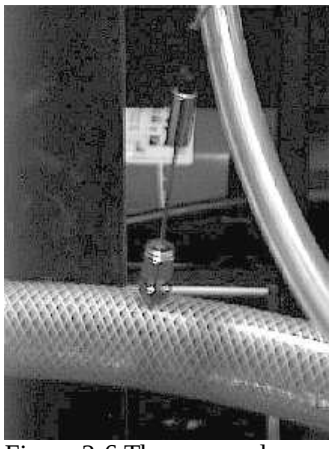
Figure 2-6 Thermocouple

2.2 Tests

The test rig was mounted on a Volvo B12 bus equipped with a Volvo TD123E engine, Appendix A. The purpose of the test rig was to be able to measure crankcase gas flow rate and oil concentration and at the same time keep track of relevant operating parameters, e.g. engine speed, torque and temperature. To get familiar with the measured data, some simple experiments were carried out. These experiments were also used to dimension the final test rig properly. In all, four different test rigs were used during the tests.

The tests on the Volvo bus were divided into different steps. The first test was the basis for the later tests. To be able to make the later tests one had to have good knowledge about the system behaviour such as the torque calculation, the signals out of the EDC unit etc.

2.2.1 Simple Flow Measurements

Only the blow-by gas flow and temperature was measured in this experiments. The engine operating conditions, including speed, gear and temperature, were noted from the dashboard instruments. The torque of the engine was estimated from the readings.

2.2.1.1 Estimation of Engine Torque

The engine torque was estimated from the roll and drag resistance of the bus. The power needed to keep a vehicle moving horizontally at constant speed is

$$P = P_{drag} + P_{roll} = AC_D\rho\frac{v^3}{2} + mgC_r v \text{ [W]} \tag{2.7}$$

where

A:	cross-section area [m^2]
C_D:	drag coefficient [-] (0.6-0.7 for buses)
C_R:	coefficient of rolling resistance [-] (0.006-0.010, truck tires on asphalt)
ρ:	air density [kg/m^3] (1.202 kg/m^3 @stp)
v:	vehicle speed [m/s]
m:	vehicle mass [kg]

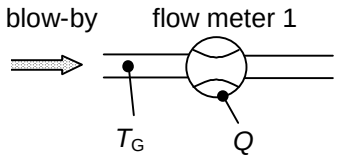

Figure 2-7 Simple flow measurement test set-up

Numerical values and equations were taken from [8].

2.2.2 Engine Operating Conditions

The purpose of this test was to estimate engine torque as described in A.2.2. The primary measurements of the test were the regulating rod voltage u_{reg}, the reference voltage u_{ref} and the engine speed N. Also, the vehicle speed was measured with radar. All signals were sampled with 10 Hz to the logger. The engine torque was estimated as described in A.2.2. The regulator rod and reference voltage were measured in the engine's EDC unit (Electronic Diesel Control). The signals from the EDC were 0 - 5 V, DC.

The engine speed signal, which was measured at the dashboard tachometer, was approximately sinusoidal. The frequency of the signal was measured with an oscilloscope and fitted to readings from the tachometer. There seems to be a linear relationship between signal frequency and engine speed (cf. Figure 2-8). We have assumed that there is no offset in the signal. The nonzero offset in the linear equation fitted to the speed and frequency measurements corresponds to a 47 rpm offset in the tachometer readings. This offset can be attributed to the course scale on the tachometer. The slope of the linear fit was used to estimate engine speed from the frequency signal as

(2.8) $N = 0.512 \cdot f$ [rpm].

The frequency signal was logged with the frequency input of the logger.

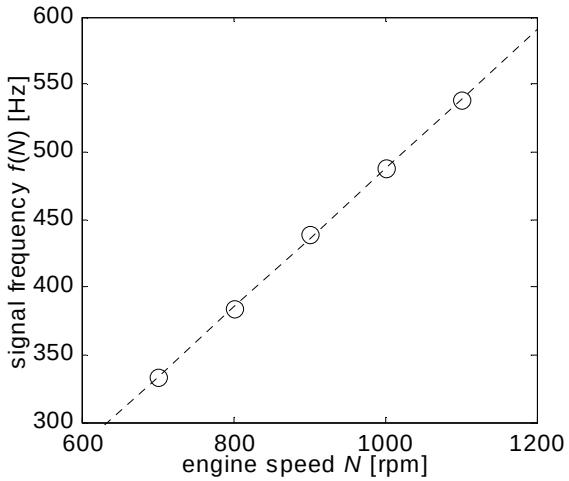

Figure 2-8 Measured engine speed signal frequency and fitted straight line: $f(N) = 0.512 \cdot N - 24.2$, $R^2 = 0.9997$

2.2.3 Stationary Size Distribution Tests

All equipment was used in this test set-up, as can be seen in Figure 2-9 and Figure 2-10. The stationary test sequence was divided into three different tests.

In the stationary concentration test, a sampling frequency of 1 Hz was considered enough. The measurements of total blow-by flow rate were made with flow meter 3, without possibility to log the values. The measurements of engine operating conditions were used to get mean values of torque and speed for the measured particle size distributions.

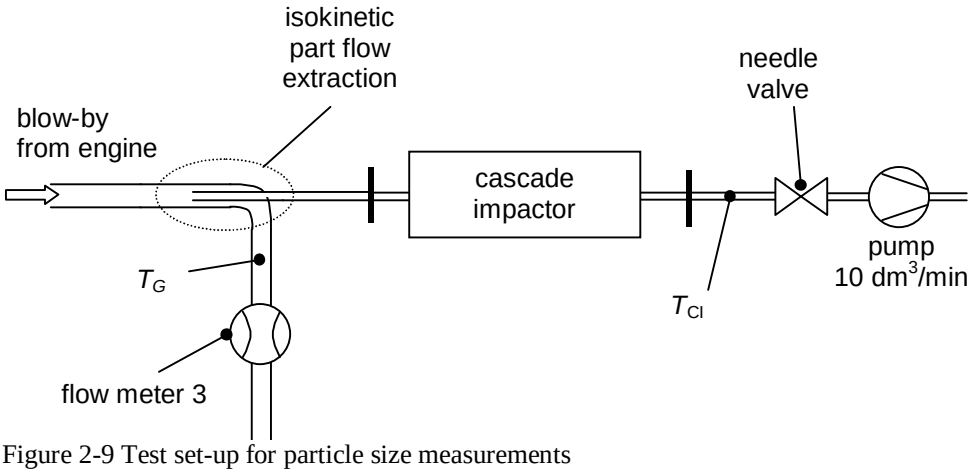

Figure 2-9 Test set-up for particle size measurements

2.2.3.1 Test 1 - Trial and Error

The first test was carried out outside LIT under supervision of Dr. Anders Gudmundsson. The test was made with idling engine. The test was used to see how big the absorbed dose of oil on the different steps in the cascade impactor was. Previous measurements indicated oil content of up to 0.5 g/m^3 in the blow-by gas. The flow rate through the cascade impactor was 10 dm^3/min. A desirable oil deposit on each foil in the cascade impactor is 0.2-2 mg. The test time of 3 min proved to be good enough resulting in oil deposits in the desired range.

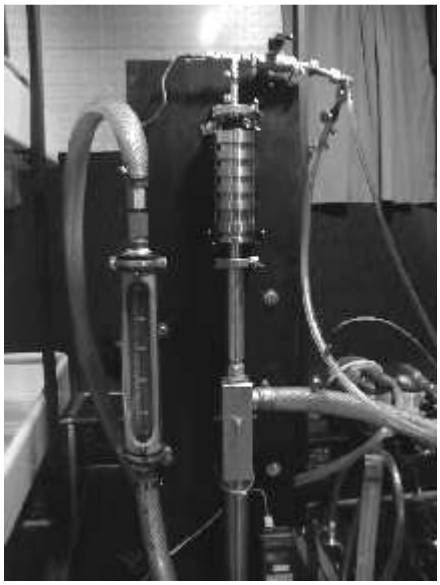

Figure 2-10 The whole particle size measuring system inside the Volvo bus. Cascade impactor (top), part flow extraction probe and flow meter 3 (left).

2.2.3.2 Test 2 - Idling With Cold Engine

The measurement on a cold idling engine was made to confirm or contradict the indication that there was less oil in the crankcase gases from a cold engine. Test duration of 3 min was used in this test as well.

2.2.3.3 Test 3 - Stationary Points According to the OICA-Standard

To verify that the amount of oil in the blow-by gases is at its maximum when the engine is working with maximum load, different test were made with the OICA-standard (cf. Appendix B) as a guide. Test durations around 1 min was used due to considerably higher oil concentration in the blow-by gas. Also, the particle size distribution with the exhaust brake active was measured.

2.2.4 Test of Flow Dynamics

The fundamental need when making a control structure is good measurement on the dynamic behaviour of the process that you wish to control. The tests on flow dynamics should be made with a sampling frequency of at least 4-10 samples per rise time to be able to reproduce the system behaviour in a simulation [4].

To be able to identify the process correctly, the system is divided into smaller independent subsystems. The crankcase gas system on the bus has been divided into three different subsystems.

- The main system, which is the *engine blow-by* flow at regular use, with the inputs engine load (torque) and engine speed.
- The second subsystem also handles the leakage around the piston rings but due to the use of the *exhaust brake* system. The input to this system is the binary exhaust brake signal (on or off) and engine speed.
- The *air compressor* is the third subsystem that can be distinguished from the whole system. The inputs we used were the engine speed and the air compressor control pressure from the air dryer. The air compressor control pressure drops from approximately 11 bar overpressure to 0 bar when the air compressor is activated. Deactivation of the air compressor is followed by a rise in the air compressor control

signal to approximately 12 bar overpressure. The air compressor control signal was converted to a binary signal indicating if the system is loading or not.

When producing data sets for one subsystem the optimum is to have as little influence as possible from the other systems, i.e. keeping engine speed constant when the air compressor and exhaust brake blow-by is investigated.

2.2.4.1 Preliminary Experiments

The preliminary experiments should be step and impulse responses [3]. These experiments can give a good idea of how the system behaves. It can be used to calculate the system gain and time constants of the system. It can also give an indication to any disturbances, non-minimum phase properties and whether or not the system is linear and time invariant. Since the engine blow-by systems is estimated to be a MISO-systems (Multiple Input Single Output) with the two input signals engine speed and engine load, there is a great importance to keep one input stable while making a step change in the other.

There is no possibility to realize an impulse in the speed or torque on a rolling bus. On the other hand, when making a step response one can differentiate the system output to estimate the impulse response of the system. Differentiation is very noise sensitive.

Earlier tests proved that climbing a hill with a variation in inclination at constant engine speed gave a good enough step in engine load. The idea to realize a step change in engine speed through shifting at constant vehicle speed (constant load) was rather difficult in practice due to the transients when shifting gear. To discern the impact of engine speed at the step response test in engine load, two different tests were made, one at 1200 rpm and one at 1500 rpm.

2.2.4.2 Blow-by Experiments

To calculate a transfer function for the system, test where the input signal varies in a large frequency range is useful. This is done under the presumption that the input signal has a lot of energy at the right frequencies, i.e. the input signal excites the system. To accomplish a good and at the same time feasible signal with a broad spectra of frequencies an acceleration of the bus slightly uphill was chosen. This gives a good variation of both engine speed and load. The resulting input signal to the system is a saw-tooth, which has an energetic content in the desired frequency range.

The exhaust brake is applied manually in the bus. This makes it controllable and it can be applied at the right time i.e. when the influence by the other subsystems are minimum. The characteristics of the exhaust brake are either on or off. The test was performed in a downhill run with several consecutive starts and stops of the exhaust brake resulting in a square wave input signal to the system. We made the assumption that the engine speed also is a controlling parameter. Engine speed should be proportional to exhaust brake blow-by if the same amount of blow-by is produced in each revolution of the engine.

The identification of the dynamics of the air compressor is simply a step response analysis, since the physical behaviour of the air compressor is either on or off.

2.2.5 Subspace Methods for System Identification

2.2.5.1 Step Response Analysis

For the identification of air compressor blow-by, a step response state space model identification Matlab® script developed by Dr. Rolf Johansson at Lund Institute of

Technology was used. The method relies on a balanced Markov parameter realization and model order reduction and is based on an algorithm developed by Juang and Pappa [19].

The Markov parameters of a system are defined as

$$H_0 = D, \quad H_k = CA^{k-1}B, \quad k = 1,2,\ldots. \tag{2.9}$$

The Markov parameters are nothing but the coefficients of the impulse response as shown below.

Let the system in (2.10) have initial states zero and let the input sequence *U* be a discrete impulse, then the output will be the set of Markov parameters in (2.9).

$$\begin{cases} x_{k+1} = Ax_k + Bu_k \\ y_k = Cx_k + Du_k \end{cases} \tag{2.10}$$

$$\begin{cases} x_0 = 0 \\ U = \{u_k\} = \begin{pmatrix} 1 & 0 & \cdots & 0 \end{pmatrix} \end{cases} \tag{2.11}$$

$$\Rightarrow Y = \{y_k\} = \begin{pmatrix} D & CB & CAB & \cdots & CA^{k-1}B \end{pmatrix} = \{H_k\}$$

■

The Hankel matrix of the Markov parameters can be factorised to the extended observability and controllability matrices as

$$H_{r,s}^{(1)} = \begin{bmatrix} H_1 & H_2 & \cdots & H_s \\ H_2 & H_3 & \cdots & H_{s+1} \\ \vdots & \vdots & \ddots & \vdots \\ H_r & H_{r+1} & \cdots & H_{r+s-1} \end{bmatrix} =$$

$$= \begin{bmatrix} CB & CAB & \cdots & CA^{s-1}B \\ CAB & CA^2B & \cdots & CA^sB \\ \vdots & \vdots & \ddots & \vdots \\ CA^{r-1}B & CA^rB & \cdots & CA^{r+s-2}B \end{bmatrix} = \tag{2.12}$$

$$= \begin{bmatrix} C \\ CA \\ \vdots \\ CA^{r-1} \end{bmatrix} \begin{bmatrix} B & AB & \cdots & A^{s-1}B \end{bmatrix} = O_r C_s$$

or more generally as

$$H_{r,s}^{(k)} = O_r A^{k-1} C_s, \; k \geq 1 \tag{2.13}$$

The rank of the extended observability and controllability matrices is smaller than or equal to the system order. Singular value decomposition of the Hankel matrix yields

$$H_{r,s}^{1} = O_r C_s = U\Sigma V^T = U\Sigma^{1/2} \cdot \Sigma^{1/2} V^T \tag{2.14}$$

from which the system matrices can be identified after eliminating the non-significant states, or rather the null space, in the singular value decomposition.

$$
\begin{aligned}
A_n &= O_n^{-1} H_{r,s}^2 C_n^{-1} = \Sigma_n^{-1/2} U^T H_{r,s}^2 V \Sigma_n^{-1/2} \\
B_n &= \Sigma_n^{1/2} V_n^T E_u \\
C_n &= E_y U_n \Sigma_n^{1/2} \\
D_n &= H_0 \\
E_u^T &= [I_{m\times m} \quad 0_{m\times(s-1)m}] \\
E_y &= [I_{p\times p} \quad 0_{p\times(r-1)p}] \\
\Sigma_n &= \mathrm{diag}\{\sigma_1 \quad \sigma_2 \quad \cdots \quad \sigma_n\} \\
U_n &= \text{matrix of first } n \text{ columns of } U \\
V_n &= \text{matrix of first } n \text{ columns of } V
\end{aligned}
\tag{2.15}
$$

where m is the number of inputs and p is the number of outputs.

Differentiation is needed when applying this algorithm to step response data. In the Matlab® script this was accomplished by applying the singular value decomposition to $H_{r,s}^{(2)} - H_{r,s}^{(1)}$ and using $H_{r,s}^{(3)} - H_{r,s}^{(2)}$ instead of $H_{r,s}^{(2)}$ in the calculation of A_n (2.15). $D_n = 0$ has been assumed in the identification procedure.

2.2.5.2 SMI-Toolbox

The State space Model Identification toolbox [12] for Matlab® developed at Delft University of Technology was used for identification of the engine and exhaust brake blow-by. The SMI-toolbox uses the *Multivariable Output-Error State Space Algorithm* (MOESP) of Verhaegen and Dewilde [19]. The algorithm is based on estimation and order reduction of subspaces somewhat similar to the method described above.

The SMI-toolbox produces a state space model of the form (2.10). Model order selection is made by inspection of singular values of the extended observability matrix, which will indicate the rank of the system if the system is observable. The algorithm provides support for multiple data sets, or batches, in the identification.

2.2.6 Measure of Model Accuracy

The variance accounted for, defined in equation (2.16), was used as a measure of model fit in the estimation of the exhaust brake and engine blow-by. The variance accounted for is the same as the coefficient of determination R^2. The VAF will be 100% if the model fit is perfect. Otherwise it will be lower.

$$
VAF = \left(1 - \frac{\mathrm{Var}(y - y_{est})}{\mathrm{Var}(y)}\right) \cdot 100\,\% \tag{2.16}
$$

3 Results

3.1 Stationary Measurement of Crankcase Gas Flow Rate

3.1.1 Warm Idling Engine

We investigated the blow-by flow at eight different engine speeds between 520 and 1500 rpm. The flow rate was approximately 40 dm^3/min at all speeds. We observed that the blow-by flow rate sometimes doubled while we were measuring. It was when the air compressor was loading the pressure air system. The measurements are shown in Table 3-1.

Table 3-1 Blow-by flow measurements on warm idling engine without air compressor

Speed [rpm]	*520*	*800*	*1000*	*1100*	*1200*	*1300*	*1400*	*1500*
Blow-by flow [dm^3/min]	45	43	43	45	37	46	37	44

3.1.2 Cold Idling Engine

The flow rate was measured at three different engine speeds directly after starting the cold engine. The EDC-unit limits the minimum engine speed to approximately 650 rpm when the engine is cold. The engine speeds that we chose were 650 (twice), 1100 and 1500 rpm. The measurements are shown in Table 3-2. The ambient temperature was approximately 10°C.

Table 3-2 Blow-by flow measurements on cold idling engine

Speed [rpm]	*650*	*1100*	*1500*	*650*
Blow-by flow [dm^3/min]	98	113	63	56

3.1.3 Loaded Engine

Since the flow measuring equipment was sensitive to inclination, the only feasible loading of the engine was air drag load and roll resistance load. By observing the engine and vehicle speed we could estimate the engine load. We had no means of measuring the acceleration of the bus. We therefore had to conduct our experiments at constant vehicle speed. We used the values $C_D = 0.65$ for air drag and $C_R = 0.008$ for roll resistance [8] in (2.7) for the estimation of engine torque.

Our objective was to keep the torque constant while varying the engine speed. However, since the gear mechanism limited the possible combinations of engine speed and vehicle speed, we could not completely fulfil our objective. The desired and estimated engine torques are tabulated in Table 3-3 together with the measured blow-by flow rate.

Table 3-3 Desired and estimated engine operating conditions and blow-by flow rate from loaded engine.

Desired engine speed [rpm]	*1100*	*1500*	*1800*	*1100*	*1500*	*1800*	*1100*	*1500*	*1800*
Desired torque [Nm]	*100*	*100*	*100*	*300*	*300*	*300*	*500*	*500*	*500*
Actual speed [rpm]	1100	1580	1800	1100	1300	1800	1150	1400	1800
Estimated torque [Nm]	82	109	124	242	294	226	410	514	444
Blow-by flow [dm^3/min]	43	52	52	51	76	55	63	76	69

3.1.4 Air Compressor

The blow-by flow from the air compressor is shown in Figure 3-1. The mean air compressor blow-by is 42 dm^3/min.

3.1.5 Blow-by Temperature

The blow-by gas temperature dependence of the engine temperature is shown in Figure 3-2.

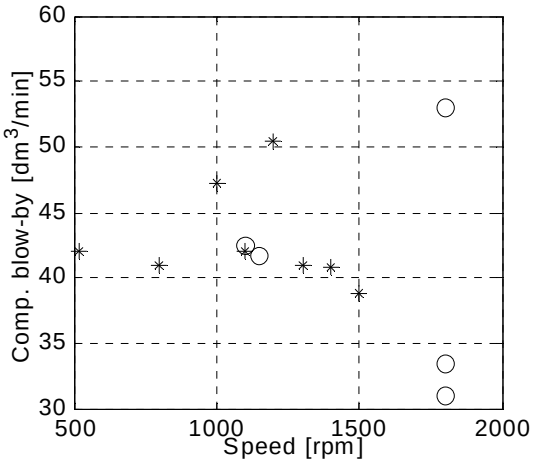

Figure 3-1 Air compressor blow-by flows from idling (*) and loaded (o) engine.

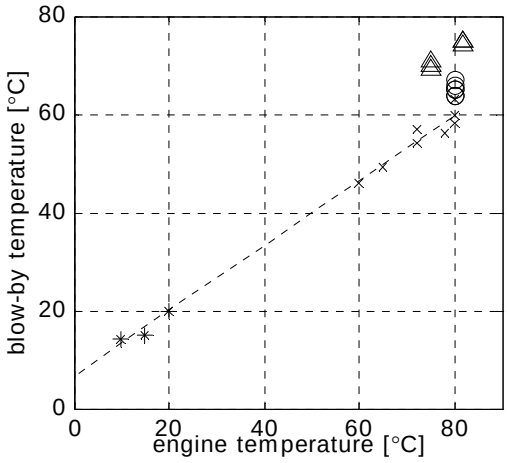

Figure 3-2 Blow-by temperature as a function of engine temperature, cold (*) and warm (x) idling and loaded engine (o and Δ)

3.1.6 All Stationary Measurements

A polynomial surface was fitted to the data from warm engine without air compressor loading (Figure 3-3). The resulting polynomial is

(3.1) $\Phi = 0.059(\pm 0.0057)N - 2.0 \cdot 10^{-5}(\pm 3.8 \cdot 10^{-6})N^2 + 0.060(\pm 0.0081)M$,

R^2 = 0.84, with estimated standard deviations in parenthesis.

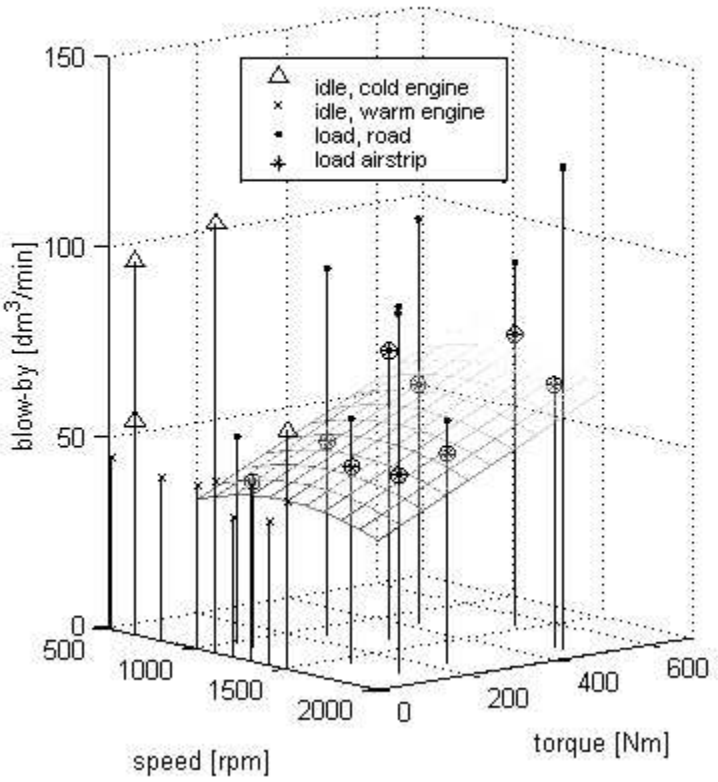

Figure 3-3 All stationary flow measurements with a surface fitted to airstrip and warm idling data. Some of the measurements include air compressor blow-by.

3.2 Dynamic Flow Rate Measurements and Identification

3.2.1 Air Compressor Loading Cycle

The data that we used for the identification of air compressor blow-by behaviour is shown in Figure 3-4. The data was recorded during idling at 1320 rpm. As seen in the figure, the blow-by during engagement and disengagement of the air compressor has different characteristics in terms of rise time. Two separate state space models have been fitted to the engagement and the disengagement of the air compressor.

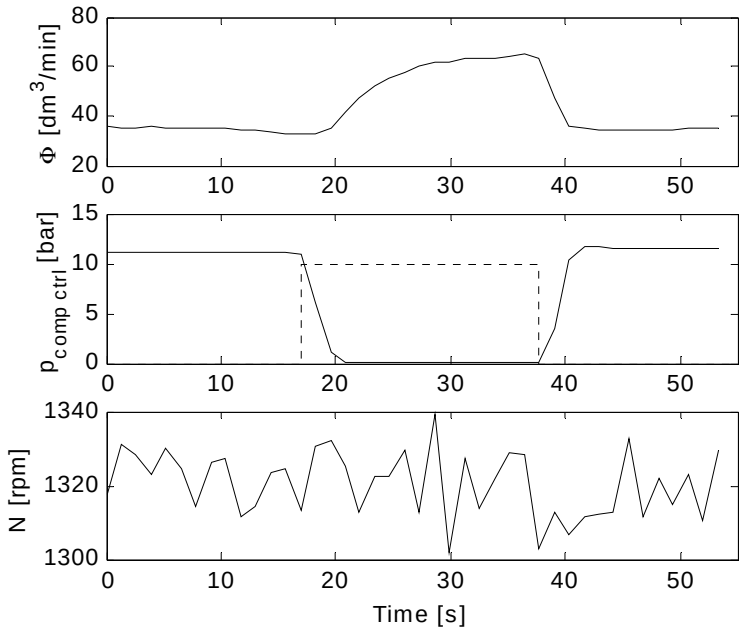

Figure 3-4 Blow-by flow during air compressor loading cycle, idling engine (top). The compressor control pressure signal from the air dryer is shown in the middle plot (solid) along with binary air compressor on/off signal (dashed).

Application of the step response algorithm described in 2.2.5.1 on the air compressor engagement data gives a second order model with real poles (figures Figure 3-5 and Figure 3-6).

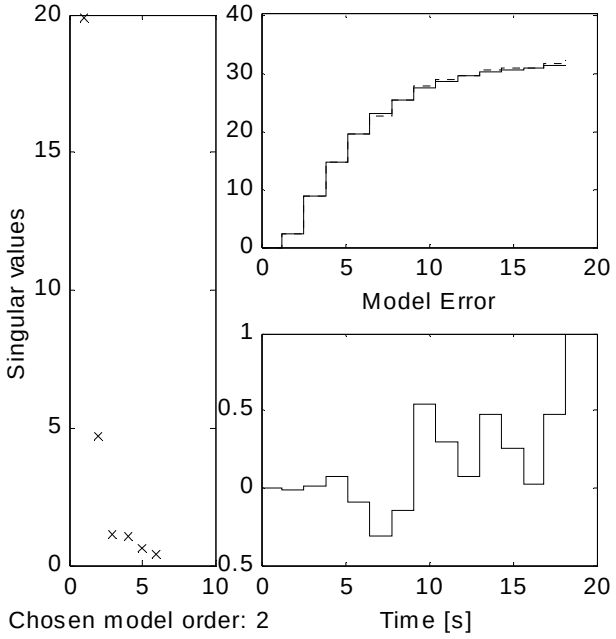

Figure 3-5 Step response data (dotted) and model step response (solid), singular values and model error from estimation of air compressor engagement.

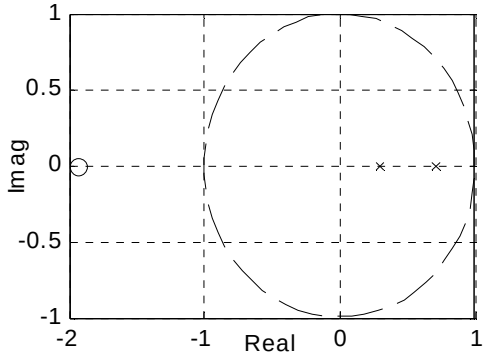

Figure 3-6 Poles and zeros of the second order air compressor engagement model. Equivalent continuous time natural frequencies: $\omega_1 = 0.26$ rad/s, $\omega_2 = 0.94$ rad/s.

The air compressor disengagement model also seems to be of order two. The resulting model has complex poles (cf. figures Figure 3-7 and Figure 3-8).

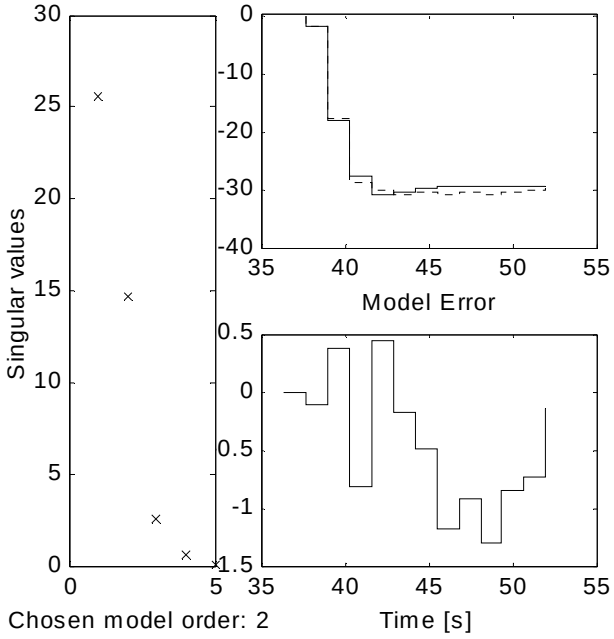

Figure 3-7 Step response data (dotted) and model step response (solid), singular values and model error from estimation of air compressor disengagement.

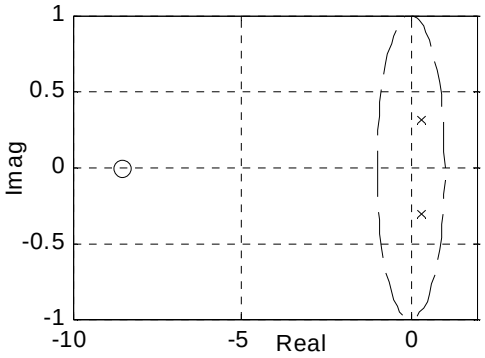

Figure 3-8 Poles and zeros of the second order air compressor disengagement model. Equivalent continuous time natural frequency and damping: $\omega = 0.88$ rad/s, $\zeta = 0.72$.

3.2.2 Exhaust Brake

The exhaust brake blow-by was identified with the SMI-toolbox. The data series used for identification is shown below in Figure 3-9. The estimated air compressor blow-by was subtracted from the data before the application of the SMI-toolbox.

There seems to be a dependence of engine speed in the data, which can be seen in the first 30 seconds of the data series. We applied two different strategies of how to handle this dependence. The first strategy was to fit a MISO state space model to the binary exhaust brake signal and the engine speed. The result from this strategy is shown in Figure 3-10. The second strategy was to divide the blow-by flow with the engine speed, hence creating a non-linear model. The result is shown in Figure 3-11.

The singular values of the extended observability matrix indicate a first order model in both the MISO and the non-linear SISO case. The VAF is about 90% in both cases.

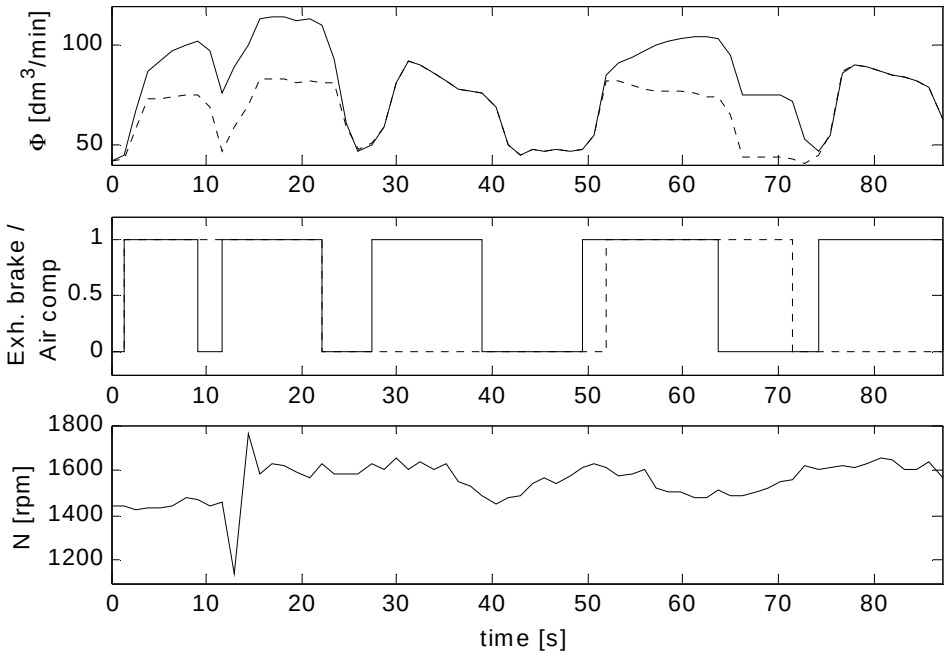

Figure 3-9 The data series used for identification of exhaust brake blow-by flow model. The dashed signal in the top plot is the measured blow-by flow minus the estimated air compressor flow. The middle plot is the binary exhaust brake (solid) and air compressor (dashed) signals.

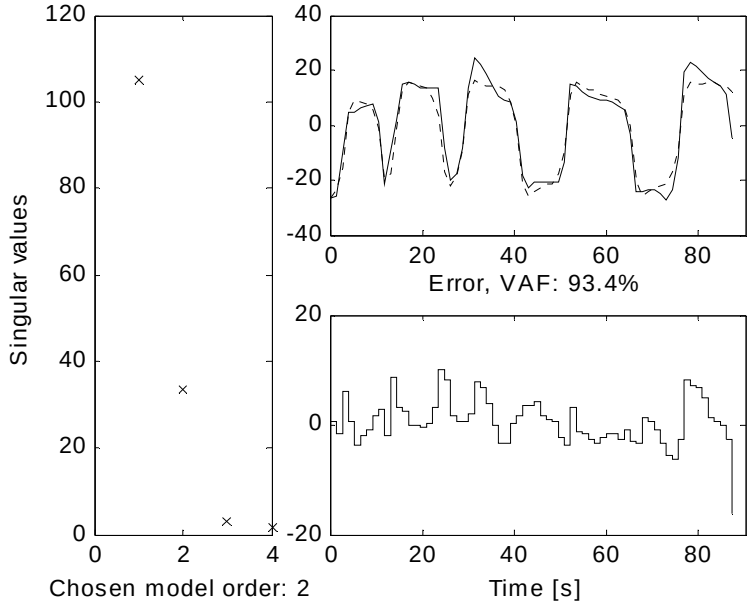

Figure 3-10 MISO model of exhaust brake blow-by flow. Input is engine speed and the binary exhaust brake signal. Equivalent continuous time natural frequency and damping: $\omega = 1.26$ rad/s, $\zeta = 0.71$.

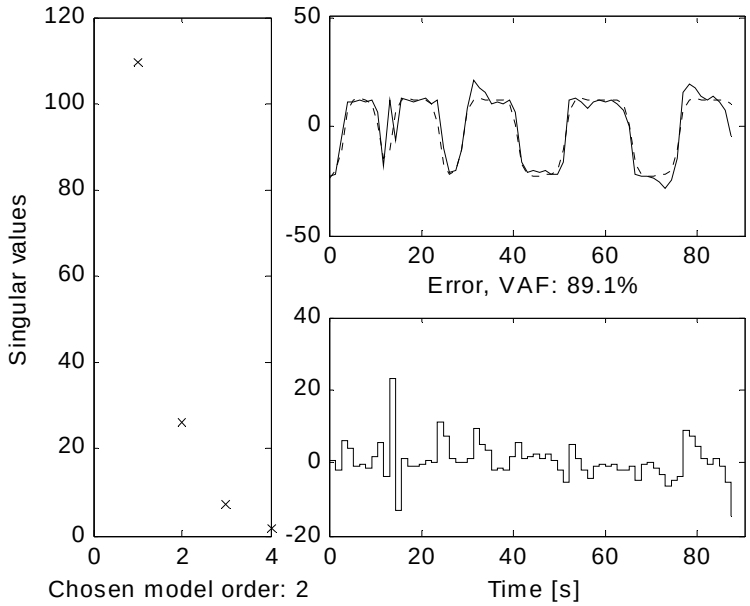

Figure 3-11 Non-linear SISO model of exhaust brake blow-by flow. Input is the binary exhaust brake signal and output is the flow q divided by the engine speed. Equivalent continuous time natural frequency and damping: $\omega = 1.26$ rad/s, $\zeta = 0.83$.

3.2.3 Engine

The engine blow-by was identified from the datasets recorded at approximately 1200 rpm and 1500 rpm respectively. Trends were removed from the data sets prior to applying the identification algorithm. The 1200 rpm identification data is shown in Figure 3-12. Judging from the data, there is a strong dependence on engine torque.

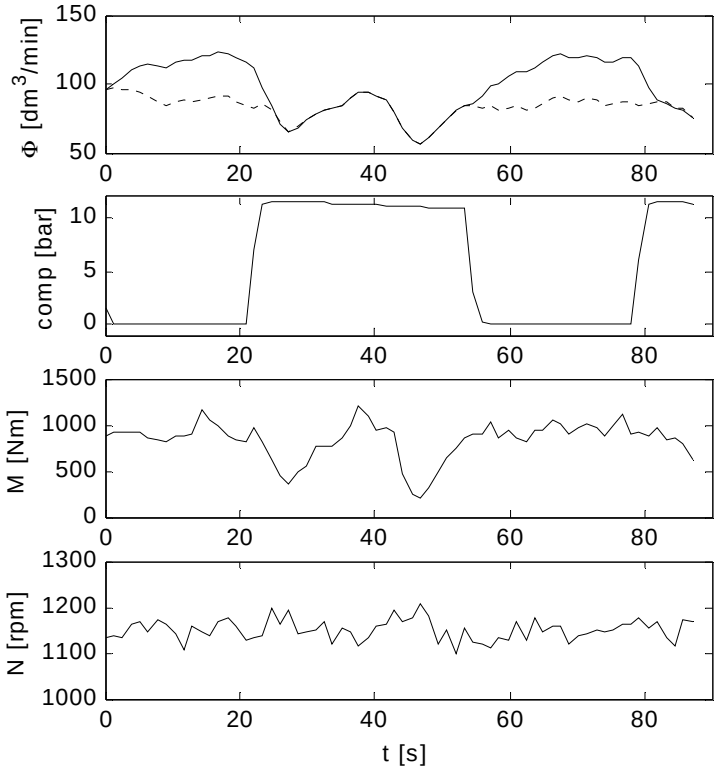

Figure 3-12 Identification data set 1 (1200 rpm). The dashed line in the top plot is the blow-by flow without air compressor blow-by.

A SISO model, with only engine torque as input, was fitted to each of the identification data sets. The model order was one in both cases. The step responses of the identified models are shown in Figure 3-13. The step responses have different magnitude.

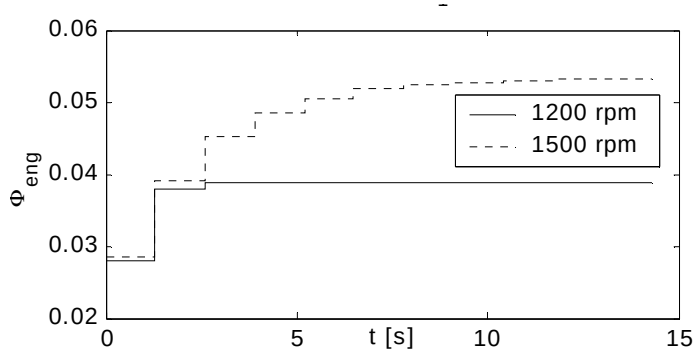

Figure 3-13 System response to step in engine torque. SISO systems identified at 1200 rpm (solid) and 1500 rpm (dashed).

MISO systems, with engine torque and speed as input, were fitted to the data to investigate if a MISO system would improve on the linearity of the estimated model. The step responses are shown in Figure 3-14.

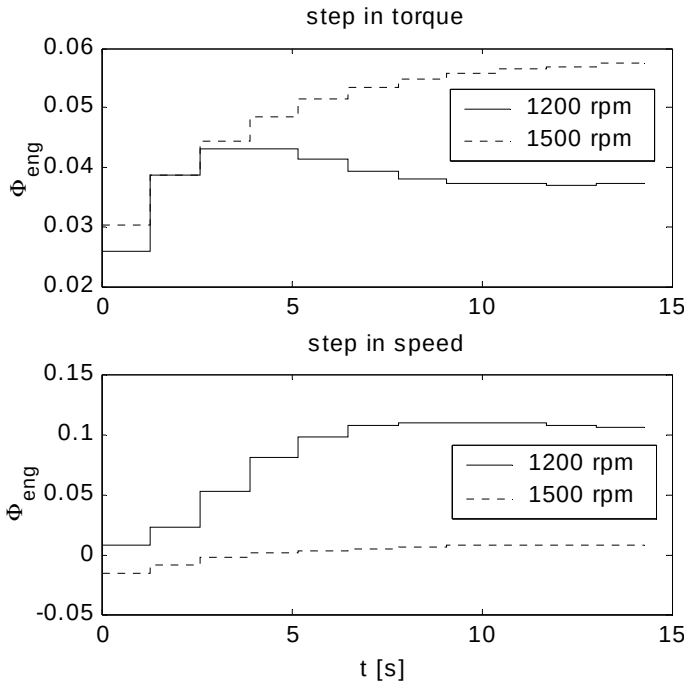

Figure 3-14 System response to step in engine speed and load. MISO systems identified at 1200 rpm (solid) and 1500 rpm (dashed).

The multiple data set feature of the SMI-toolbox was used to fit a common model for the two data sets. The results, along with singular values and validation data, are shown in Figure 3-15.

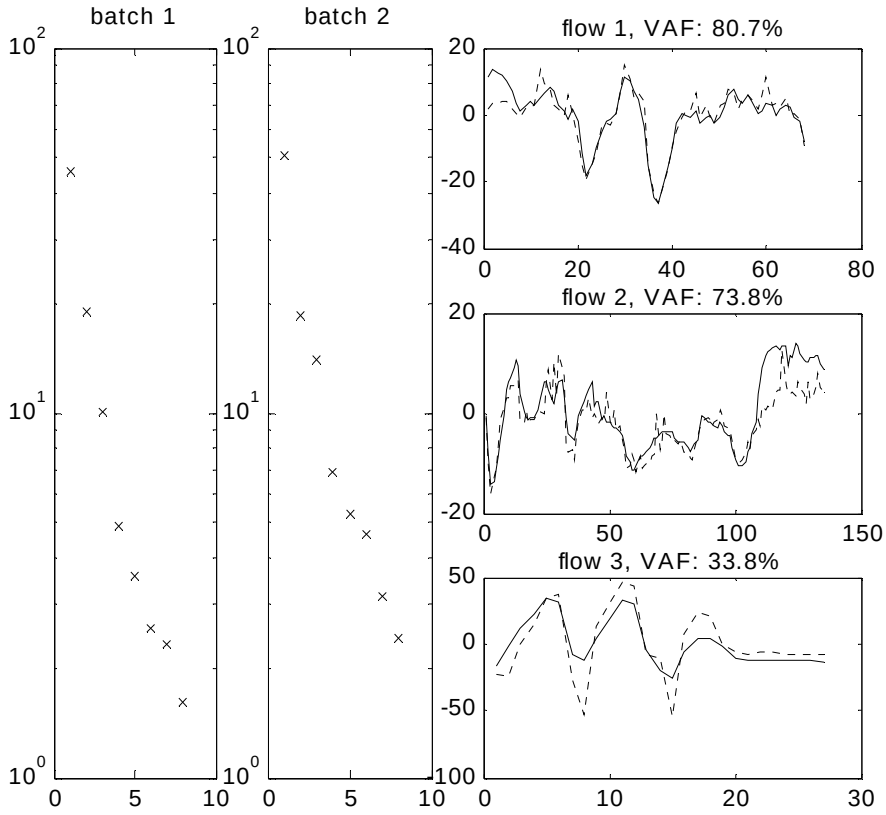

Figure 3-15 Singular values from multiple data sets MISO identification. Identification data is in top two plots and validation data in bottom right. The dashed curves are estimated blow-by. The estimated model is of order 1.

For comparison a polynomial surface was fitted to the engine speed, load and blow-by data. This corresponds to a zero order dynamic model, i.e. a static model. The resulting polynomial is

(3.2) $\Phi = 0.044(\pm 3.9 \cdot 10^{-4})N - 0.054(\pm 2.9 \cdot 10^{-3})M + 1.5 \cdot 10^{-5}(\pm 2.9 \cdot 10^{-6})M^2$,

R^2 = 0.82, with estimated standard deviations in parenthesis.

3.2.4 Simulation

The simulations were performed in Simulink® with the identified models of engine, exhaust brake and air compressor blow-by. The static model of engine blow-by was used in the simulations. Engine torques <0 Nm were interpreted as 0 Nm in the simulations.

In the first simulation, shown in Figure 3-16, the engine speed and load is in the same region as the identification data sets. In the other three simulations, Figure 3-17 to Figure 3-19, either the engine speed or load is outside of the range of the identification data. The simulated results show an offset compared to the measured data.

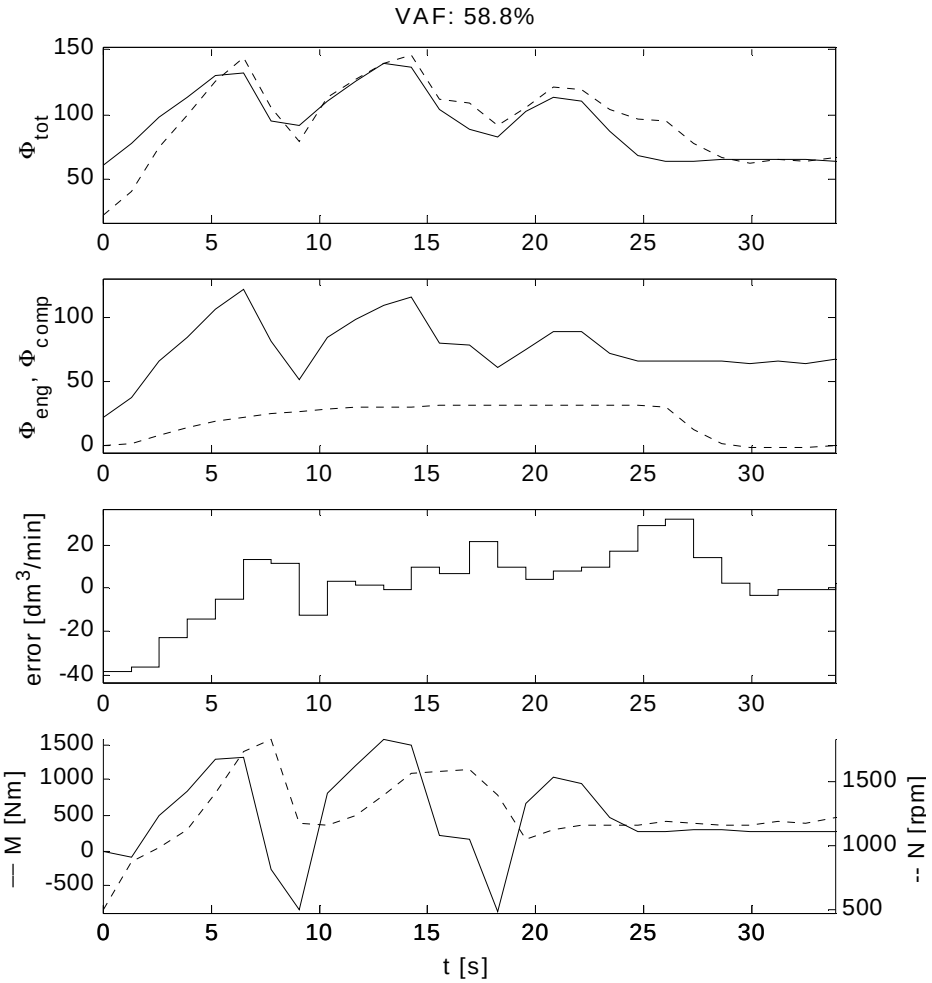

Figure 3-16 *Uphill acceleration*. Simulation of entire blow-by system with zero order MISO model for engine blow-by. The top plot shows real (solid) and simulated (dashed) flow. The second plot is the components of the blow-by: engine (solid) and air-compressor (dashed).

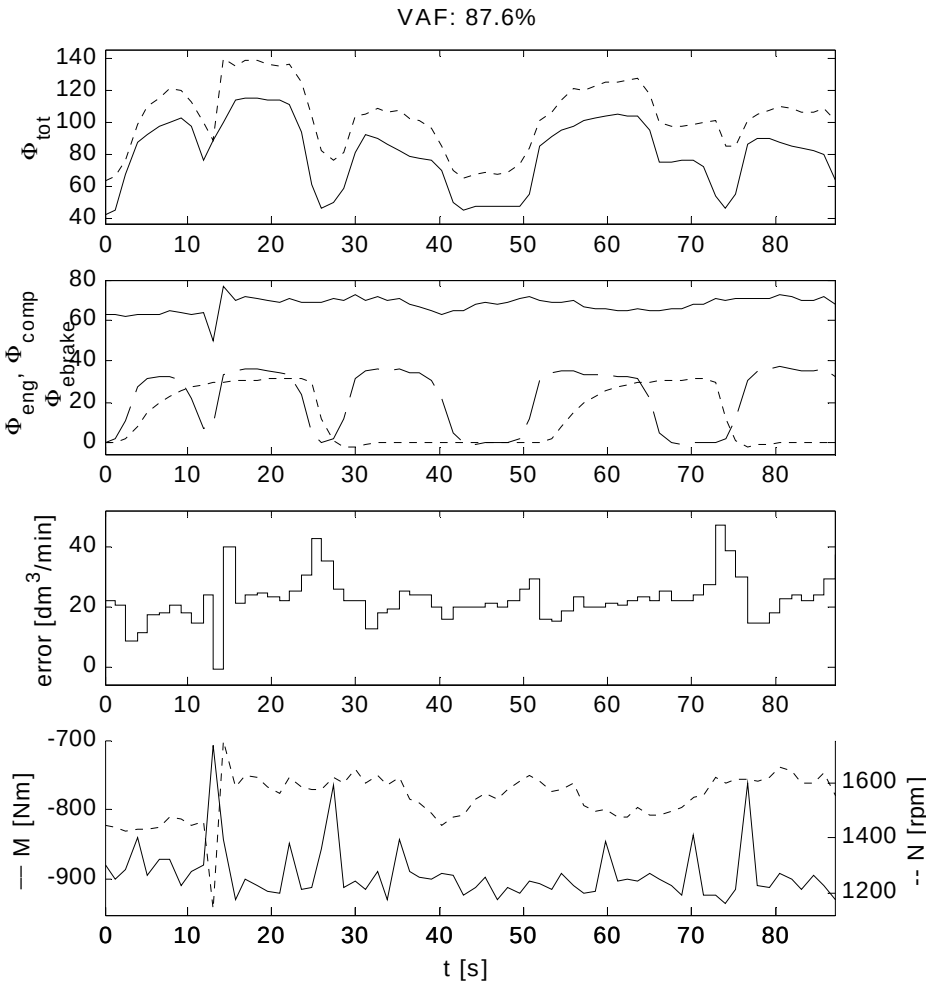

Figure 3-17 *Exhaust brake*. Simulation of entire blow-by system with zero order MISO model for engine blow-by. The top plot shows real (solid) and simulated (dashed) flow. The second plot is the components of the blow-by: engine (solid), air-compressor (dashed) and exhaust brake (dash-dotted).

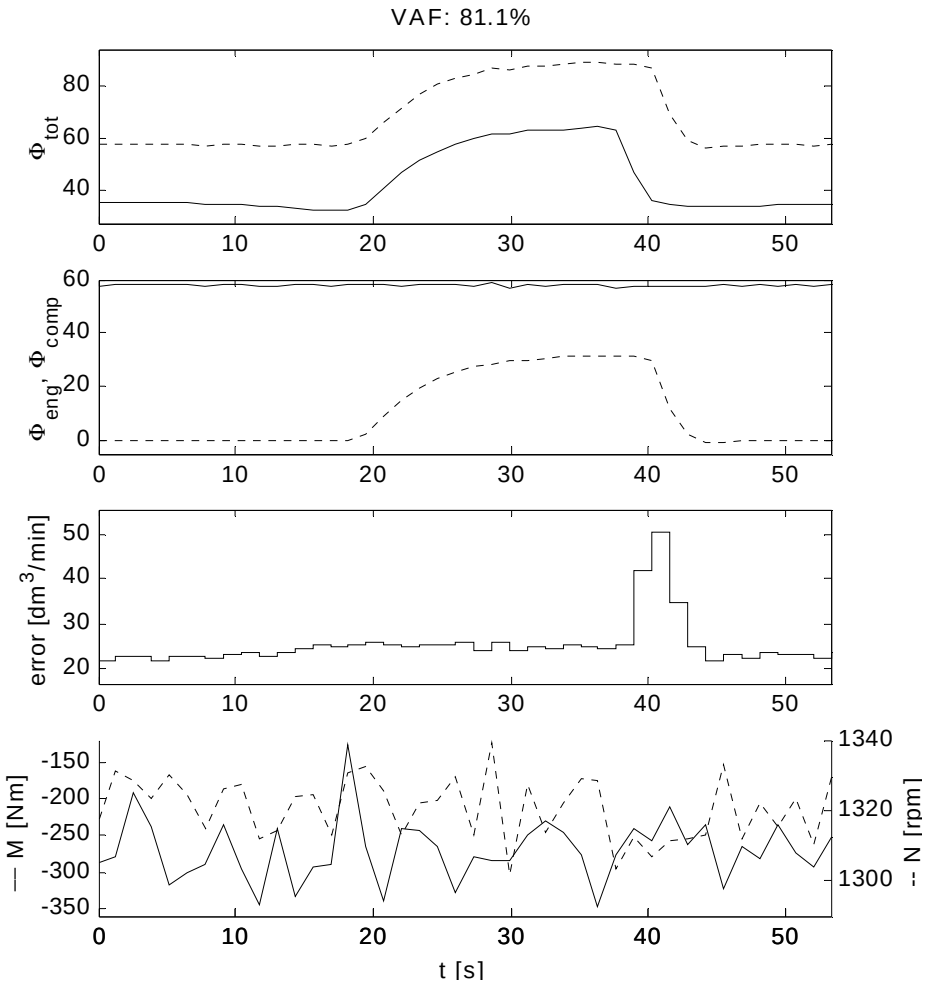

Figure 3-18 *Air compressor, high idle.* Simulation of entire blow-by system with zero order MISO model for engine blow-by. The data was recorded at high idle (1300 rpm). The top plot shows real (solid) and simulated (dashed) flow. The second plot is the components of the blow-by: engine (solid) and air-compressor (dashed).

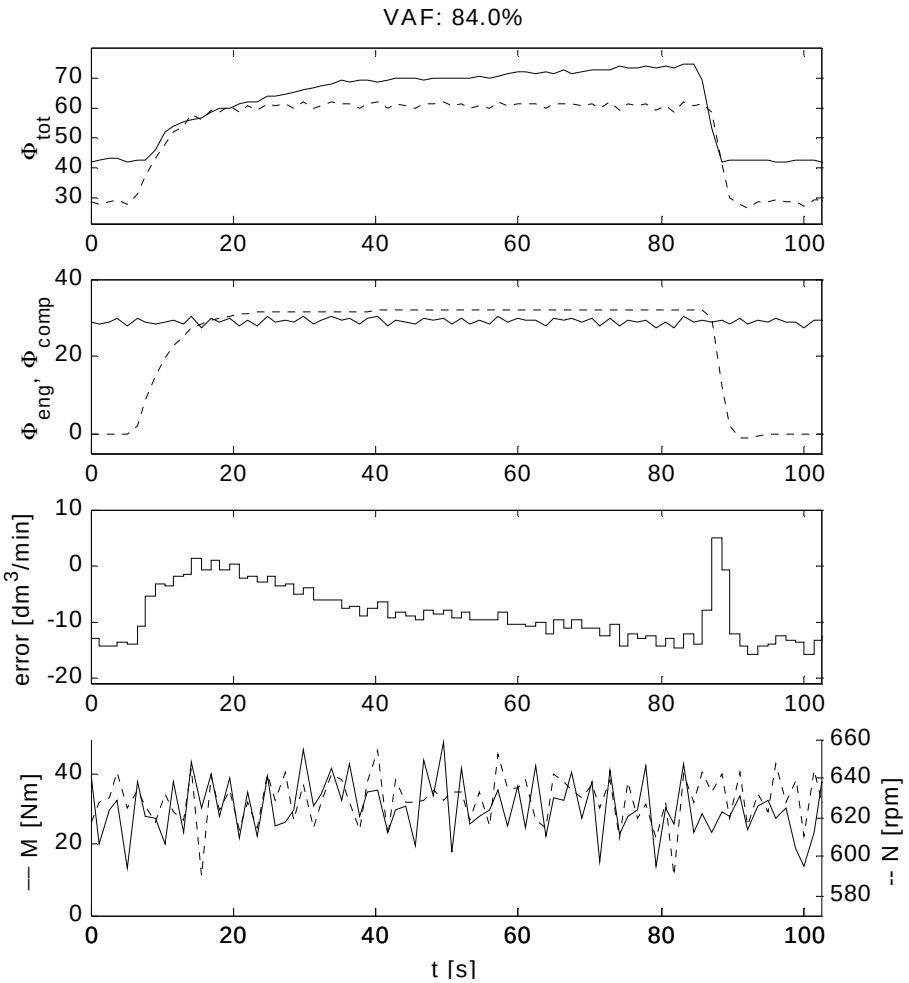

Figure 3-19 *Air compressor, low idle.* Simulation of entire blow-by system with zero order MISO model for engine blow-by. The top plot shows real (solid) and simulated (dashed) flow. The second plot is the components of the blow-by: engine (solid), air-compressor (dashed) and exhaust brake (dash-dotted).

3.3 Particle Size Distribution

The particle size distribution was measured at eight different operating conditions. The resulting distributions are shown in Figure 3-20 to Figure 3-22. Each point in the diagrams shows the portion of the particles that are smaller than the size given on the X-axis. Figure 3-23 shows the total amount of oil in the blow-by aerosol in all different tests.

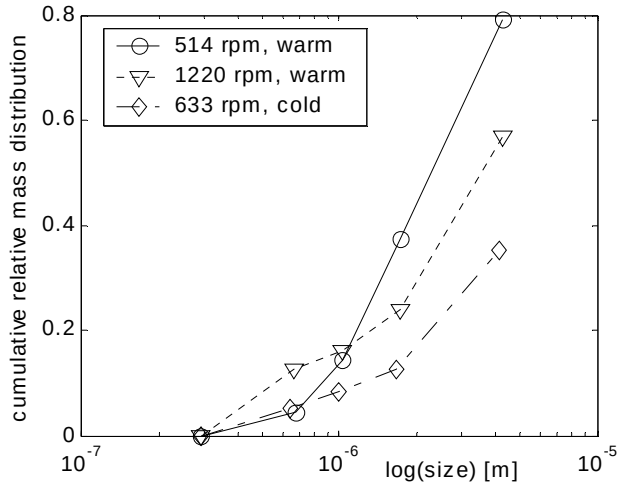

Figure 3-20 Size distribution, warm and cold idle.

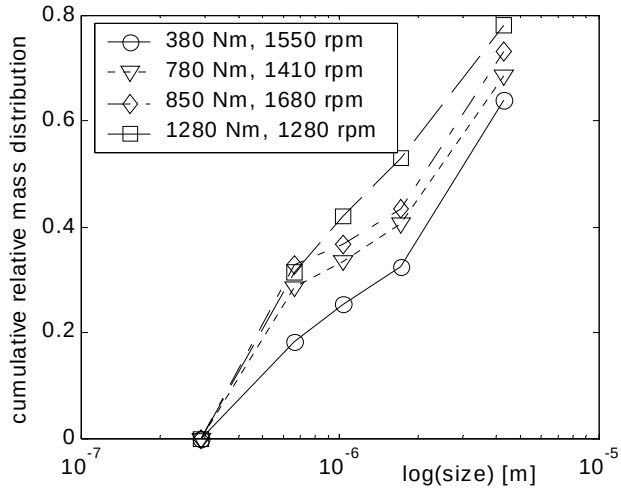

Figure 3-21 Size distribution, different engine torque and speed.

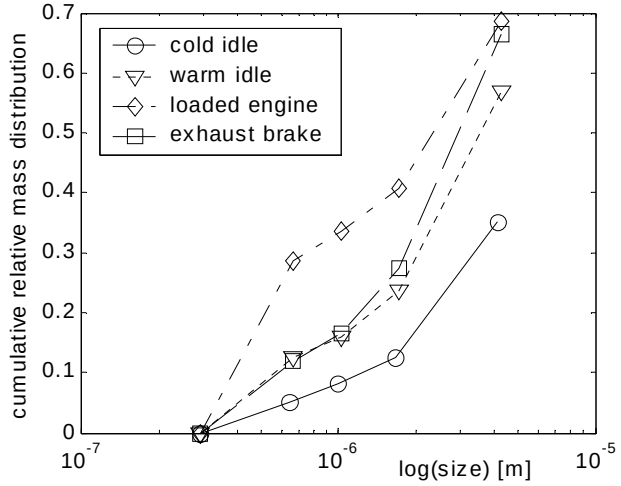

Figure 3-22 Size distribution, comparison of exhaust brake, idling and loaded engine

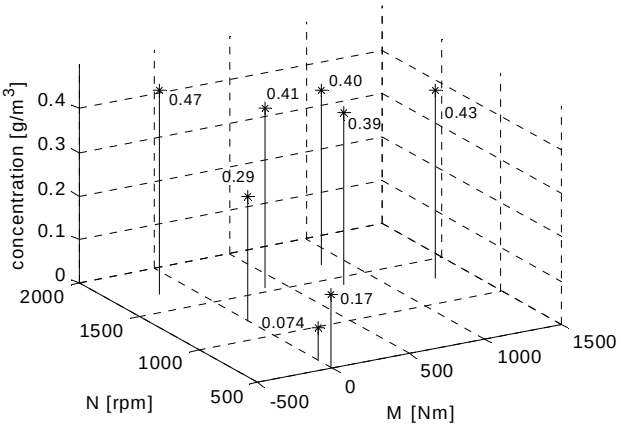

Figure 3-23 Total oil concentration in blow-by. Exhaust brake has the highest concentration and cold engine has the lowest concentration.

4 Comments

4.1 Stationary Measurement of Crankcase Gas Flow Rate

4.1.1 Idling Engine

There seems to be no dependence of the engine speed in the blow-by flow rate on idling engine. The idling blow-by flow rate is around 43 dm^3/min at all speeds. The measurements on cold engine were probably corrupted by the air compressor, with blow-by flows of about 100 dm^3/min in the first tests at 650 and 1000 rpm and approximately 60 dm^3/min in the following tests (cf. Table 3-2). There seems to be a considerable increase in the blow-by flow rate when the engine is cold (almost 50 % increase).

4.1.2 Loaded Engine

The blow-by flow rate is highest in the middle engine speed range and there is a tendency of increasing blow-by flow with increasing engine torque.

The choice of C_D and C_R was not verified experimentally or by any other means. Nor was the possible effect of wind taken into account. The estimated engine torque is only to be seen as an indication of the real torque.

At the highest estimated torques, approximately 500 Nm, the vehicle speed was almost 90 km/h. The bus speed was electronically limited to 90 km/h. The maximum torque of the engine was 1600 Nm. To be able to test the engine in its full range of operating conditions, we had to put extra load on the engine by braking the bus in some way, increasing the bus weight or by going uphill.

4.1.3 Air Compressor

There is no clear dependence of engine speed in the air compressor blow-by in the stationary flow rate tests as shown in Figure 3-1. This is an indication that the air compressor loading is a linear system in terms of magnitude.

The air compressor pressure is dependent on the pressure in the pressure air system. Increasing pressure in the air system gives increasing pressure in the air compressor. Hence, the air compressor blow-by should be different at different stages in the pressure air loading cycle. This is verified in the dynamic tests of air compressor blow-by (cf. 3.2.1). An explanation of the large variance at high engine speed in Figure 3-1 might be that the measurements have been made at different points in the pressure air loading cycle.

The amount of blow-by from the air compressor is equal to the engine blow-by at idle.

4.1.4 Blow-By Temperature

The measurements of blow-by temperature verify that the gas temperature is closely related to the engine temperature. Higher load also gives higher temperature, possibly since the transport time delay of the gas is shorter due to higher flow rates.

4.1.5 All Stationary Measurements

The degrees of the estimated polynomial ($\deg(N) = 2$, $\deg(M) = 1$) are the highest degrees for which all polynomial coefficients are statistically significant. No intercept has been included in the estimated polynomial, since there should be no blow-by when the engine is not revolving. However, since the data points are very few and the estimation of the

torque is quite uncertain, no conclusions regarding the blow-by behaviour or linearity of the system should be drawn at this stage.

Polynomials fitted to data are poor predictors outside of the range of the data used for identification. As can be seen in Figure 3-3, the surface will clearly underestimate the blow-by at low engine speeds.

4.2 Dynamic Flow Rate Measurements and Identification

4.2.1 Data Pre Processing

The flow rate signal was sampled with sampling period 1.275 s and all other signals were sampled with sampling period 1.3 s. The flow rate data was resampled with linear interpolation to get the same sampling period in all data series. Linear interpolation has some low-pass characteristics since it removes some of the peaks in noisy data.

There was no synchronization between the flow measurements and the other signals. By matching the air compressor engagement and disengagement to the flow data, a coarse synchronisation was accomplished, without consideration of any possible intersample shift. Poor synchronization and intersample shift will lead to poor estimates of the system poles and zeros, possibly introducing non minimum-phase characteristics. This leads to considerable uncertainty as for how to interpret the results of the dynamic flow measurements.

4.2.2 Air Compressor Loading Cycle

When the loading of the pressure air system starts, the piston compressor cylinder is pressurized and put in contact with the pressure air system via a non-return valve. In the beginning of the pressure air loading the pressure rise in the system is fast. The higher the air system pressure, the lower the pressure rise rate. The air compressor blow-by flow rate seems to mimic the behaviour of the pressure in the pressure air system.

When the air compressor is disengaged, the pressure in the cylinder of the piston compressor immediately drops to atmospheric pressure. This can explain the difference in rise time in the engagement and disengagement behaviour of the air compressor blow-by flow.

The sampling period of 1.3 s is reasonable for modelling the engagement of the air compressor, but too long to model the disengagement. A sampling frequency of at least 2 Hz would be preferable.

Engine speed influences the air compressor blow-by as can be seen in the simulation in Figure 3-19. A model with engine speed as additional input would probably be more accurate in describing the air compressor blow-by.

4.2.3 Exhaust Brake

The engine speed clearly influences the exhaust brake blow-by flow in some way, making it necessary to use a MISO system of some kind to model the exhaust brake blow-by. The normalized flow shown in Figure 3-11, where the flow has been divided by the engine speed, has equal magnitude in each of the exhaust brake engagements and disengagements.

The identified models have equal speed and are well damped. Judging from the graphs, there is some fast dynamics that the model doesn't catch. The sampling period is too long for good modelling of the exhaust brake system.

4.2.4 Engine

The engine blow-by system is clearly non-linear as seen in Figure 3-13 and Figure 3-14. The fact that a static model can reproduce the output with as much accuracy as the dynamic models indicate that the dynamics in the engine blow-by formation is much faster than the sampling period at 1.3 s. This is quite easy to understand since the engine response to accelerator pedal is usually much faster than 1.3 s.

The singular values shown in Figure 3-15 show no clear model order. The reason for poor behaviour of the singular values can be a low signal to noise ratio or non-linearity in the system [12]. The poor synchronisation of the sampling could also be a reason that the system order is hard to determine. The model accuracy in the validation is quite poor.

There is a problem in the estimation of engine torque and blow-by related to torque. The calculation of engine torque described in A.2.2 produce negative torques when the engine is idling at high speeds and also when there is no fuel injection in the engine. There is in fact a negative torque involved when the vehicle motion drives the engine via the crankshaft (e.g. motor brake), but this torque should have no influence on the blow-by behaviour since there is no extra combustion chamber pressurization associated with it. A more detailed mapping from engine speed and regulator rod position to engine torque is needed to produce valid estimations of engine torque.

4.2.5 Simulations

The identified models seem to follow the system quite well when the engine speed and torque is in the same range as the identification data as in Figure 3-16. Problems arise from the negative torque (Figure 3-17 and Figure 3-18) and low engine speed (Figure 3-19) in the input data. The engine blow-by estimation has the wrong level.

There is a problem in the estimation of the air compressor disengagement, which is always a couple of samples too late compared to the real system. This leads to an overestimated air compressor flow each time the air compressor is disengaged. This problem is due to the simulation in Simulink and can easily be corrected for in an implementation of the air compressor simulation.

The air compressor engagement system seems to depend on engine speed. The measured air compressor blow-by has slower dynamics than the estimated in Figure 3-19. The disengagement has the same characteristics at both high and low engine speed.

4.3 Particle Size Distribution

A word of caution is needed before interpreting the particle size distribution and concentration measurements. The total amount of oil in the blow-by is quite uncertain since we had no end filter after the cascade impactor. Particles that are smaller than the smallest cut-off diameter in the impactor (0.29 μm) could very well contribute to the overall mass concentration. The lack of end filter also affects the measured size distribution. The leftmost points in the size distribution figures should be shifted upwards by the amount of oil that is captured by the end filter (cf. (2.6)).

Figure 3-21 indicates that high torque give smaller particles. There might also be a change towards smaller particles when the engine speed is increased. The shift towards smaller particles could be an effect of higher flow velocities in the leakage around the piston rings due to high cylinder pressure and greater atomisation of the lubricating oil film.

When the exhaust brake is active, the particle size distribution is almost the same as from the idling engine. There is no fuel injection when the exhaust brake is active and the pressure in the combustion chamber is fairly low. The flow velocity around the piston rings is small, possibly leading to less atomisation than in the high torque case.

A cold engine produces considerably less small particles than a warm engine. This is probably due to the high viscosity of cold engine oil. There is also less vaporization of light fragments of the engine oil leading to less formation of aerosol from condensation.

Both engine speed and torque seem to influence the overall oil concentration in the blow-by gas. The highest oil concentration was measured when the exhaust brake was active. A cold engine produces less oil aerosol than a warm engine.

With some knowledge about the physical dimensions of the crankcase, conclusions can be drawn about the transport delay of the oil droplets in the blow-by gas.

5 Conclusions

5.1 Blow-By Modelling

The tests made in this master thesis only determine the characteristics of the particular engine at hand, Volvo TD123E. Modern engines have higher cylinder pressure and probably higher engine blow-by. The particle size distribution can also vary a lot in the interesting region around 1 μm [20]. Engines with similar design will probably have similar blow-by behaviour, which will facilitate the modelling of blow-by.

The system identification made in this master thesis project shows that it is possible to simulate crankcase gases with a model based on the inputs speed and torque. There are however some fast dynamics, which are not caught by the models. These dynamics could probably be included if the sampling rate was increased. There is no kind of age or wear parameter that describes the effect of total operating time on the system, which could be introduced to make it valid over a longer term. To make this possible, additional tests on the same engine after a predetermined distance must be made. The different systems could then be weighted together with gain scheduling or interpolation. The system temperature dependence is not investigated either.

Our choice of subsystems seems to be a reasonable way to handle the whole system. Since the air compressor and, in some way, the exhaust brake are external sources that affect the amount of blow-by independent of the engine in normal operation, it is natural to identify them separately. As mentioned earlier it would however be preferable with a higher sampling rate when identifying these systems. The fast dynamics during the disengagement of the air compressor is clearly not modelled in a proper way. The exhaust brake also has some dynamics that are not included in the model, which can depend on the sampling ratio or perhaps on some other phenomenon. In addition to the increased sample rate the importance of a common clock is clear, since a misfit in the synchronization of the different sampled systems may introduce an unstable zero.

There are different solutions of the exhaust brake on the market. These might have different blow-by characteristics both in terms of flow and oil content. Other engine models might have additional auxiliaries or components that generate blow-by.

The blow-by from the air compressor is independent of the engine. There only seems to be a few major manufacturers of air compressors for heavy-duty vehicles. Models of the available air compressor's blow-by could be made separate from models of engine blow-by.

The particle size distribution shows that the amount of smaller particles increases with higher torque. There are also some indications that smaller particles accrue with higher engine speed. This means that the separator characteristics and in particular the cut-off size is of great importance and hence the next thing inline that should be investigated. The tests also show that the exhaust brake gives the highest amount of oil concentration in the blow-by gases. This could be a general trend that holds for all engines but it should be verified by tests on other models before it is stated.

There can be no conclusions drawn about a general dynamic behaviour of engine blow-by from this master thesis project. Additional test must be made to confirm the indications that this thesis gives.

5.2 Design of Control System

The parameters that determines the degree of separation in the separator is fluid flow, particle size, rotational speed and, to a very small extent, the gas temperature (cf. C.2.2). The only parameter that can be controlled is the rotational speed of the separator.

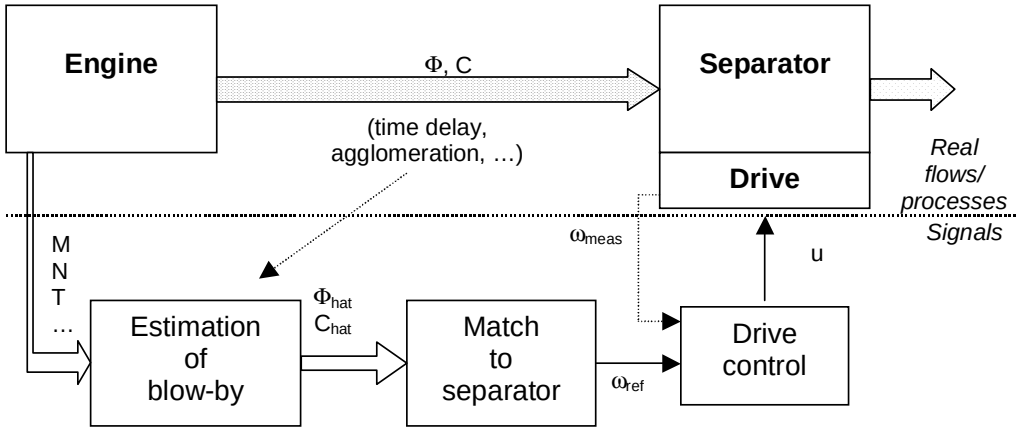

Figure 5-1 Structure of an open loop control system for the crank case oil separation system.

5.2.1 Open vs. Closed Loop Control

When controlling the separator without any sensors, the use of an accurate model of crankcase gases is critical. These models can only be developed by testing every engine model individually and build up a system for each model that the cleaning device should be mounted on. If physical models of the engine was made one could yield on the demands on engine tests, but this only holds if proper physical models can be developed and verified.

A solution that would make the identification procedure unnecessary is the possibility to have a sensor of some kind and to measure the amount of gas flow. This is a very simple solution if the right sensor can be found, both out of an economical and practical perspective. We have not investigated the sensors available one the market any further. One possibility would be a hot-wire. However, there is still a need for particle size measurements if only a flow sensor is introduced.

The optimal solution for the control of the separator is to have a sensor for the oil amount as well. Then the separator could be controlled in closed loop to work at an optimum operating point regarding to the concentration of oil and the flow rate of the gas.

5.3 Recommendations on Future Work

The most important things for Haldex and Alfa-Laval in a nearby future is to:

- Characterize the separator properly. The efficiency must be known in form of cut-off size at a given rpm and flow rate to be able to make a control of the Alfdex possible.
- Make a test routine that is used both by Alfa-Laval, Haldex and perhaps also involved customers. When testing the separator knowledge about the size distribution of the oil mist as well as the flow rate is fundamental.
- The possibility to introduce sensors of flow or oil content in the separator should be investigated.

Methods for measuring particle size distribution of aerosols in real time exist. Time saving would be one of the advantages of real time online measurements of size distribution. The entire cascade impactor procedure of mounting and weighing the filters is both time-consuming and prone to error. Real time measurements would also make it

possible to investigate the effects of the transport of the aerosol from the crankcase to the separator.

As for the flow measurement equipment, the influence of the pulsations in the blow-by flow rate on the flow measurements should be investigated.

Independent of which way the project develops in the future, towards open loop control or if a suitable sensor is found, a specification of proper testing of every new engine that should be equipped with the Alfdex separator must be done. The tests are needed either in order to tune a controller for the scenario with sensors, or to make the identification and develop a controller in the case where the gas flow should be modelled. The extent of these tests could of course be discussed and adjusted to the desired accuracy of the controller.

6 References

[1] Abstract from the standard, ISO 8573-4:2001(E)

[2] Alfa-Laval educational material

[3] Andersson, A, et al; A Manual for System Identification; Course material in System Identification course, Department of Automatic Control, Lund Institute of Technology 2002

[4] Åström, Karl J., Wittenmark, Björn; Computer Controlled Systems Theory and Design, third edition; Prentice Hall, Inc, Upper Saddle River 1997, ISBN 0-13-314899-8

[5] Barris, Marty, Closed Crankcase Filtration, http://www.meca.org/crankcasearticle.html (January 2003)

[6] Batram, Bernhard, Brunsmann, Ingo, Knickmann, Kai-Uwe; Oil Mist Separators – The Next Generation; Hengst Filterwerke, Münster, 2000.

[7] Bischof, O, Tuomenoja,H; The Measurement of Blow-by Gas Particles; (Accepted for publication in MTZ 7-8/2003)

[8] Bosch Automotive Handbook, 5th ed.; Robert Bosch Gmbh, Stuttgart 2000; ISBN 0-8376-0614-4

[9] Busen, Jürgen, Kein, Michael, Pietschner, Sieghard; Development Partner Hengst; Hengst Filterwerke, Münster, 2002

[10] Chang-Yu, Wu; Lecture notes from Aerosol Mechanics course; Dept. of Environmental Engineering Sciences, University of Florida; www.ees.ufl.edu/homepp/cywu/ENV6130/Single.ppt (October 2002)

[11] Gudmundsson, A; Characterisation of Samplers for Estimation of Aerosol Exposure; Licentiate Thesis, Division of Working Environment, Lund Institute of Technology; Lund 1994

[12] Haverkamp, B, Verhaegen, M; SMI-toolbox version 1.0 manual; Systems- and Control Engineering Group, Delft University of Technology, Delft 1997

[13] Heisler, Heinz; Advanced engine technology; Butterworth-Heinemann, Oxford, U.K. 2001; ISBN 0-340-56822-4.

[14] Heywood, John B.; Internal combustion engine fundamentals; McGraw-Hill Book Co, Singapore 1988; ISBN 0-07-100499-8.

[15] http://www.dieselnet.com/standards/cycles/esc.html (January 2003)

[16] http://www.vv.se/publ_blank/bokhylla/miljo/handbok/ (January 2003)

[17] Interview with Lars Erlandsson, M. Sc.; Reliability & Durability, Volvo Truck Corporation

[18] Johansson, B; Förbränningsmotorer, del 1; Institutionen för värme- och kraftteknik, Lunds Tekniska Högskola, Lund 2002

[19] Johansson, R; System Modelling and Identification; Prentice Hall, NJ 1993; ISBN 0-13-482308-7

[20] Krause, W; Ölabscheidung in der Kurbelgehäuseentlüftung; Dr.-Ing Dissertation, Fachbereich Maschinenwesen, Univ. Kaiserslautern; Kaiserslautern 1995

[21] Marjamäki, M et. al.; Performance Evaluation of the Electrical Low-Pressure Impactor (ELPI); Journal of Aerosol Science, vol. 31, no 2, pp 249-261, 2000

[22] Sauter Hartmut L[a]., Lenz Tomas A[a]., Zink Alexander[b], A New Effective and Lifetime Oil Mist Separator for Crankcase Ventilation Systems, [a]Mahle Filtersysteme GmbH, [b]Institut für Mechanische Verfahrenstechnik University Stuttgart, Stuttgart, Germany

[23] Sauter, H.L., Trautmann, P.; Messung und Abscheidung von Ölnebelaerosolen aus der Kurbelgehäuseentlüftung von Verbrennungsmotoren; MTZ, 61 (2000) 12, pp. 874-878

[24] Volvo service manuals

[25] www.epa.gov, US Environmental Protection Agency

[26] Young, Hugh D., Freedman, Roger A.; University Physics, 9th Edition; Addison-Wesley Publishing Company, USA 1996; ISBN 0-201-31132-1

Appendix A The TD123E Engine

The TD123E engine is a 12 litres 6 cylinder inline turbocharged diesel engine. The engine was manufactured by Volvo in 1995. It uses a direct fuel injection system with a row injector pump and it has an intercooler. The injection system is electronic (EDC Electric Diesel Control) with 6-nozzel injectors at each cylinder.

A.1 Specifications

Type TD123E
Maximum Power.....262 kW (356 bhp) @1900 rpm (32 r/s)
Maximum Torque .....1600 Nm @1200 rpm (20 r/s)
Number of Cylinders.....6
Bore.....130,17 mm
Stroke .....150 mm
Volume.....12,0 dm^3
Compression Ratio.....17,8:1
Compression Pressure .....3100 kPa @220 rpm (3,7 r/s)
Maximum speed at full load .....1900 rpm (32 r/s)
Low idle.....530 rpm
Air compressor.....Knorr LP49, 600 cm^3 piston compressor

Note: The engine used in the experiments was a prototype so deviation from above can exist. The engine is quite old, but it has not been extensively used. The normal service life of heavy-duty vehicles is around 900.000 km. Our bus had rolled 150.000 km.

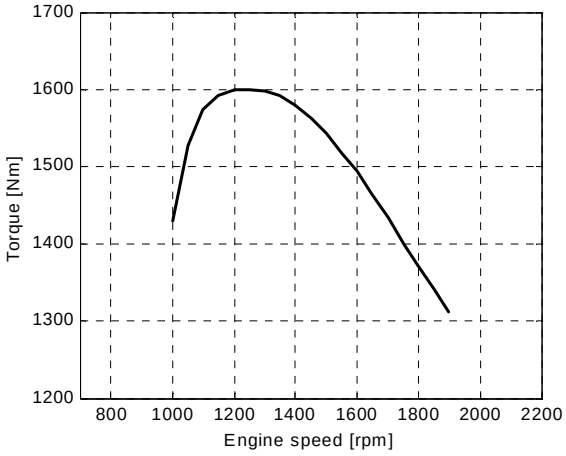

Figure A-1 Estimated torque (TD123E)[1]

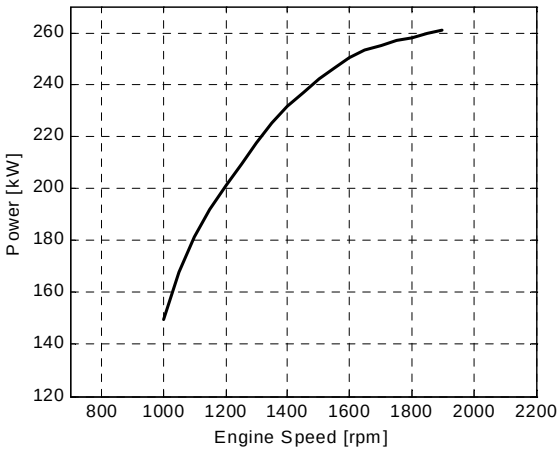

Figure A-2 Estimated power (TD123E)[1]

A.2 EDC-Unit

The Electronic Diesel Control unit on the TD123E engine control the position of the regulating rod of the row injector pump. The position of the regulating rod determines the amount of fuel that is injected in each combustion cycle. The row injector pump is

[1] The estimation is made by copying the curve from the service manuals [24].

described in more detail in [18]. The regulating rod position can be extracted from the EDC-unit as a 0-5 V test signal for testing purposes. There is also a reference voltage in the EDC-unit for normalisation. The measured regulating rod voltages have to be normalized with the reference voltage according to

(A.1) $$u_{reg}^{norm} = 5\frac{u_{reg}}{u_{ref}} \text{ [V]. [24]}$$

A.2.2 Estimation of Engine Torque

The maximum and minimum of the regulating rod voltage has to be measured and normalized prior to estimating the regulating rod position. Regulating rod minimum occurs when the only load on the engine is the friction load, i.e. pumping load, engine rubbing friction load and load by engine auxiliaries [14]. This corresponds to idling. The maximum of the regulating rod occurs at maximum engine load. The regulating rod position can be then estimated by the linear expression

(A.2) $$rod = \frac{u_{reg}^{norm} - u_{\min}}{u_{\max} - u_{\min}} \in [0,1].$$

By assuming a linear mapping from regulating rod position to engine torque M, an estimate of the engine torque is

(A.3) $$M = rod \cdot M_{\max}(N) \text{ [Nm]}$$

where $M_{max}(N)$ is the engine maximum torque as a function of engine speed as seen in Figure A-1.

A.3 Air Compressor

The Knorr LP49 air compressor is a piston compressor. The speed of the piston compressor is greater than the speed of the engine. It has two states, on or off, which are controlled by the air dryer. The air dryer engages the piston compressor when the pressure in the pressure air system drops below a certain pre-set limit. The air compressor is disengaged when the air pressure reaches the desired pressure.

The air compressor is mounted on the engine and the crankcase of the air compressor is in conjunction with the engine crankcase. The service life of common air compressors (approx. 300.000 km) is shorter than the service life of engines and the degradation of performance is significant. The air compressor is changed two to three times in an engine lifetime.

A.4 Exhaust Brake

The exhaust brake is a system for vehicle safety and economy complementing the wheel brakes. The basic principle is to increase the pumping losses (cf. [14] or [18]) of the engine. This can be accomplished by blocking the tail pipe or by changing the valve lift strategy.

A.5 Turbocharger, Intercooler and Turbo Compounder

The turbocharger uses the energy in the exhaust gases to increase the pressure in the inlet manifold. The exhaust gases powers a turbine mounted after the exhaust manifold. The exhaust turbine shaft is coupled with a compressor turbine in the inlet, which increases the pressure in the inlet. The turbocharger turbines are matched for optimum performance in the working range of the engine.

Cooling of the air in the intake manifold further increases the density of the inlet air, enabling higher volumetric efficiency. The intercooler, also called aftercooler, is a heat exchanger mounted after the inlet turbine.

A turbo compounder is a way to use the excess power in the exhaust gases. It is a turbine with direct coupling to the engine crankshaft adding extra torque to the engine. The TD123E is not equipped with turbo compounder.
[14]

Appendix B The OICA Standard

The OICA standard [15] is used for certification of heavy-duty diesel engines. The standard have been used in Europe since the year 2000. The test uses 13 different test modes, which are weighted together trough the weight factors seen in Table B-1. The engine is tested in a dynamometer and all modes are at steady state. The engine is tested trough the whole cycle with no interrupt while changing mode, and the first 20 seconds of each mode is used for stabilizing and changing speed and load. The maximum deviations from the modes are for speed ±50 rpm and for torque ±2 % of the maximum torque at the test speed.

Table B-1 OICA-Standard

Mode	*Engine speed %*	*Load %*	*Weight factor %*	*Time*
1	Low idle	0	15	4 min
2	25	100	8	2 min
3	50	50	10	“
4	50	75	10	“
5	25	50	5	“
6	25	75	5	“
7	25	25	5	“
8	50	100	9	“
9	50	25	10	“
10	75	100	8	“
11	75	25	5	“
12	75	75	5	“
13	75	50	5	“

The ranges that the standard is based on is 25-100 % of the engine torque and the three different speed modes are chosen as 25, 50 and 75 % of a specified area seen in Figure B-1. The area is determined by the limits n_{low} and n_{high}, which are specified as

- n_{low} is the lowest speed where the power output is 50 % of the declared maximum net power.
- n_{high} is the highest speed where the power output is 70 % of the declared maximum net power.

In addition there are three random test points within the test area.

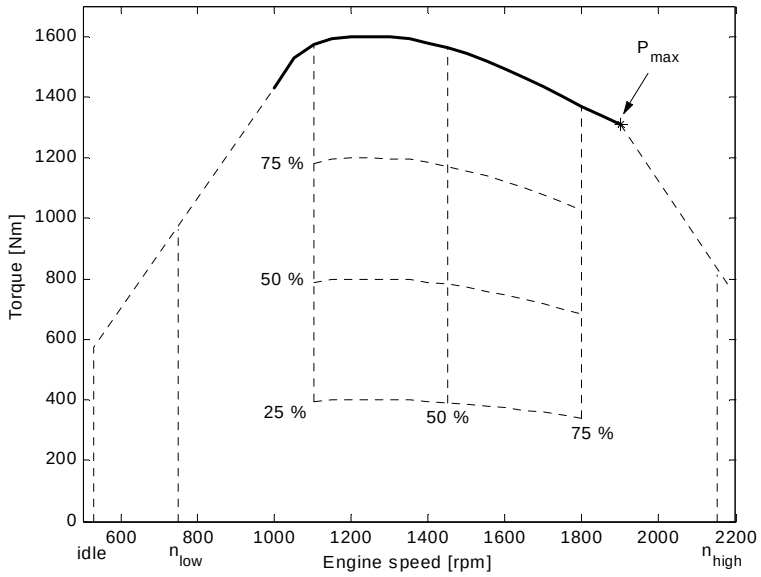

Figure B-1 Estimated torque on the TD123E engine, with the OICA standard applied.

Appendix C The Disc Stack Separator

The separator was invented by Gustaf de Laval in 1877 and was initially used for separating cream and milk. Today, applications range from oil separation to pharmaceutical applications.

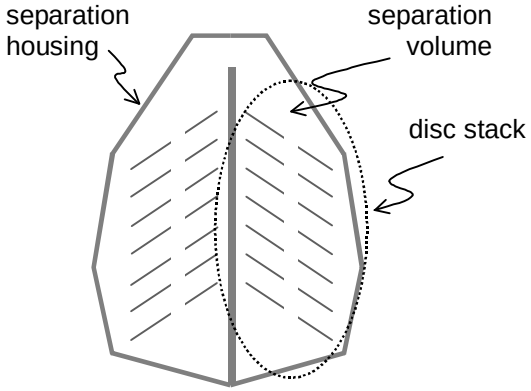

Figure C-1 Separator terminology

C.2 Basic Construction

The main part of a disc stack separator is inside the separation housing. In the housing a number of conical discs are stacked on top of each other forming the separation volume. A mixed fluid is fed to the separation volume in which it separates into its components.

C.2.1 Operating Principle

A particle in a viscous fluid is influenced by three principal forces (cf. Figure C-2). According to Archimedes principle, the buoyancy force F_b is proportional to the mass m of the displaced fluid. Gravitational force F_g is proportional to the particle mass m'. Stokes law gives the drag force F_d of a sphere with relative velocity v in a viscous fluid if the flow around the sphere is laminar (C.3). If the flow is turbulent (C.4) holds. However, the flow around the oil droplets in the separator can be considered to be laminar [2]. The equations for a spherical particle are shown below. [26]

(C.1) $$\overline{F}_b = -m\overline{g} = -\frac{\pi d^3}{6}\rho\overline{g}$$

(C.2) $$\overline{F}_g = m'\overline{g} = \frac{\pi d^3}{6}\rho'\overline{g}$$

(C.3) $$\overline{F}_d = -3\pi\eta d\overline{v}\text{ , laminar flow}$$

(C.4) $$\overline{F}_d = -C_D A\frac{\rho\overline{v}^2}{2}\text{, turbulent flow}$$

These forces can be combined to give the terminal speed of a sphere falling in a liquid:

(C.5) $$\overline{v}_T = \frac{(\rho'-\rho)d^2}{18\eta}\overline{g}$$

The basic principle of a separator is to alter the gravitational acceleration g by rotating the particle-fluid system. (C.5) is replaced by (C.6). By adding a suitable continuous flow Φ of the fluid, particles of different density and shape will move in different directions. Dense particles will move towards lager radii and light particles towards the centre (cf. Figure C-3 and Figure C-4).

(C.6) $$\bar{v}_T = \frac{(\rho' - \rho)d^2}{18\eta}\omega^2\bar{r}$$

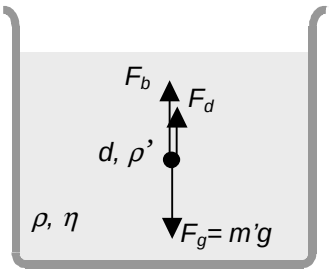

Figure C-2 Forces acting on a particle with density ρ' and diameter d in a viscous fluid of density ρ and viscosity η.

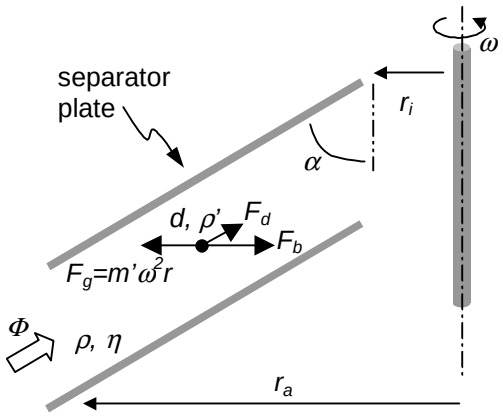

Figure C-3 Forces acting on a particle in a rotating system with a fluid flow Φ.

Holes in the discs distribute the mixed fluid so that all discs will be a part of the separation volume. After passing through the separator, the light component of the fluid can be extracted from the centre of the separation volume and the heavy component on larger radii.

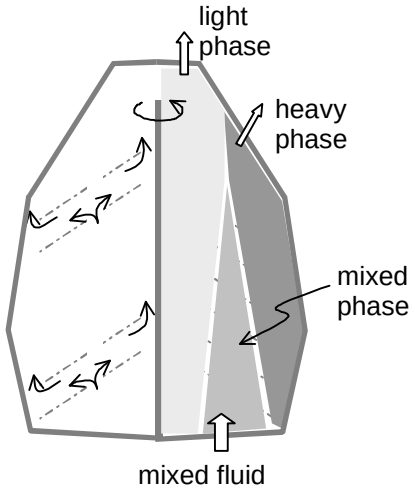

Figure C-4 Flow and distribution of fluid in a basic separator

C.2.2 Theoretical Cut-Off Size

The following equation describes the minimum droplet size, which can be completely separated using a separator constructed as in Figure C-3.

(C.7) $$s = \frac{1}{\omega}\sqrt{\frac{27\eta_g \tan(\alpha)\Phi}{\pi(r_a^3 - r_i^3)(\rho_f - \rho_g)}}$$

where

Φ: volume flow
η_g: viscosity of the gas
ρ_g : density of the gas
ρ_f : density of the fluid

r_a, r_i, and α is constructional parameters seen in Figure C-3. The equation is taken from [22]. The tests made by [22] shows that the real degree of efficiency is better than the calculated one.

C.3 The Alfdex 160 Oil Mist Separator

The Alfdex 160 separator is a gas separator. The equations stated above still holds, but the viscosity and the density of a gas are much lower than those of a liquid. The terminal velocity of a particle in a gas will therefore be much higher. It is no longer possible to separate different components of the gas but it is possible to rid the gas of larger particles and droplets.

The contamination in the crankcase gas mainly consists of oil droplets of different sizes and constitution. These droplets hit the discs and form an oil film on the discs, which continuously flows towards larger radii. At the edges of the discs, the oil film is thrown onto the housing wall and led to the oil outlet and back to the oil sump.

Since the gas is fed to the centre of the separation volume, the Alfdex 160 separator also works as a centrifugal pump with a small pressure increase from inlet to outlet.

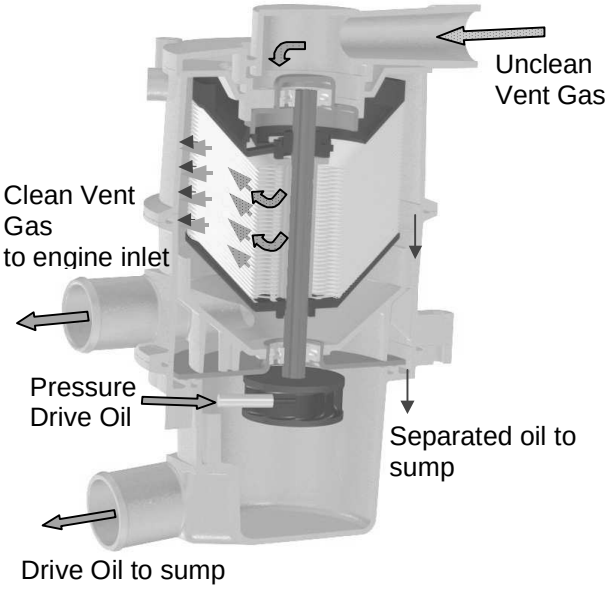

Figure C-1 Alfdex 160 crankcase gas separator